Getting

continuous, recirculating flow

on a

3D blood-vessel-on-chip

integrated on a

fluidic circuit board

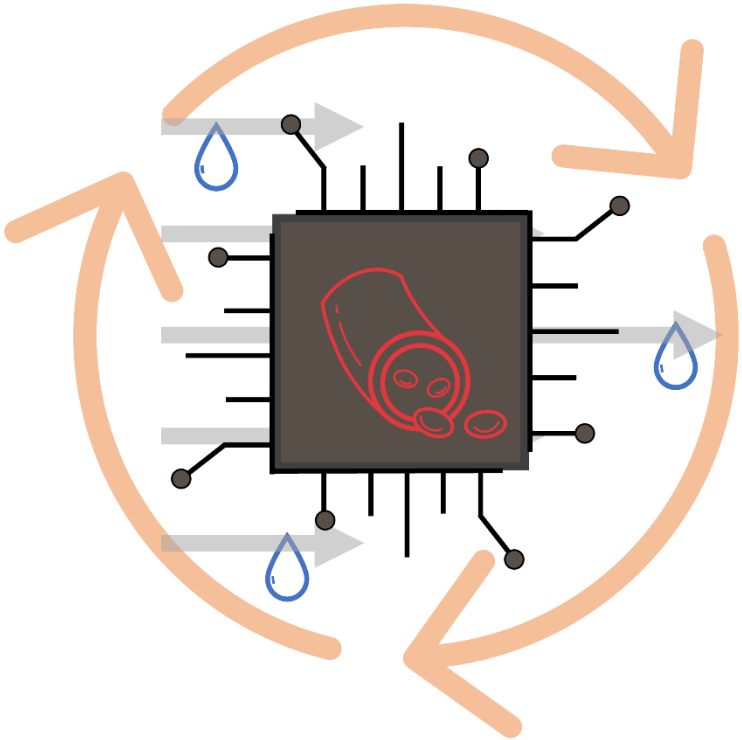

Meike Große-Elshoff

UNIVERSITY OF TWENTE.

MASTER'S THESIS

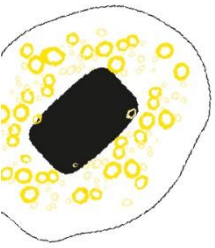

M. Große-Elshoff BSc.

March 14, 2023

Graduation Committee

H. H.T. Goosen-Middelkamp, MSc

dr. A.R. Vollertsen

Prof. dr. A.D. van der Meer

Prof. dr. ir. M. Odijk

Prof. dr. ir. S. Le Gac

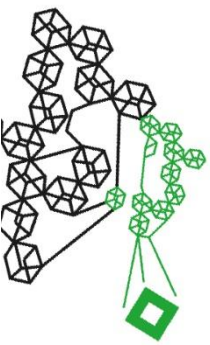

BIOS Lab-on-a-chip Group

Applied Stem Cell Technologies

Biomedical Engineering – Bioengineering Technologies

Faculty of Electrical Engineering, Mathematics and Computer Science
Faculty of Science and Technology

University of Twente

Enschede, the Netherlands

TECHMED CENTRE

Abstract

Blood-vessel-on-chips (BvoCs) are being developed to study plaque development and rupture. Until now, these models have failed to combine essential *in vivo* aspects such as continuous reperfusion, parallelization, 3D vessel structure, and physiological shear. However, these aspects are needed to establish a realistic *in vitro* model to study plaque development and rupture. A main reason hampering research using Organ-on-Chips (OoCs) such as BvoCs is the lack of standardization and modularity that impede the translation of OoCs to industrial and clinical settings. To overcome the shortcomings of OoCs, fluidic circuit boards (FCBs) are being developed. FCBs are microfluidic platforms having well plate dimensions and a standardized interface that allow the integration of components such as valves and pumps in a plug-and-play fashion, resulting in one modular platform.

This thesis presents the design of a FCB and of modular building blocks (BBs). BvoCs with viscous finger patterned (VFP) 3D lumen seeded with human umbilical vein endothelial cells (HUVECs) were used. To the best of our knowledge, connecting chips with VFP channels with a FCB was only developed once. Therefore, one of the project's challenges was to design the interface between chips with VFP channels and FCB so that the VFP lumen and the cell-lumen integrity remain intact. Blunt needles were used as interfacing methods, and BvoCs were connected to mini-FCBs. Using this method and applying a shear of 3.1 Pa, the lumen and most of the cell-lumen integrity remain intact. In addition, it is believed that the further extension of the standardization approach in OoC research will enable easier collaboration due to the interchangeability between BBs. Using the designed FCB and modular BBs to introduce continuous recirculation on parallelized VFP BvoCs can be a valuable addition to the research on plaque development and rupture. In future research, adding predefined inlets to the chip mould can further improve the interface between BvoCs and FCB. Moreover, gradually increasing flow rates can improve cell alignment and lead to uniform monolayers. In addition, adding multiple cell types and patient material can bring research one step closer to the in vivo situation, reducing animal testing, enabling personalized medicine, and decreasing drug failure rates.

Samenvatting

Bloedvaten-op-een-chip (blood-vessel-on-chips, BvoCs) worden ontworpen om de ontwikkeling van plaque en plaque ruptuur te bestuderen. Tot nu hebben deze modellen gefaald om essentiële *in vivo* aspecten zoals continue reperfusie, parallellisatie, 3D vaatstructuur, en fysiologische afschuiving te combineren. Echter zijn deze aspecten nodig voor een realistisch *in vitro* model, voor het bestuderen van plaque-ontwikkeling en ruptuur. Een van de belangrijkste redenen die het onderzoek met organ-on-chips (OoCs) zoals BvoCs hindert is het gebrek aan standaardisatie en modulariteit die het vertalen van OoCs naar de industrie en kliniek belemmert. Om de tekortkomingen van OoCs te overwinnen worden fluïdische printplaten (fluidic circuit boards, FCBs) ontwikkeld. FCBs zijn microfluïdische platen met afmetingen van celkweekplaten en een gestandaardiseerde interface. De interface maakt de integratie van componenten zoals kleppen en pompen op een plug-and-play manier mogelijk, resulterend in één modulair platform.

Deze studie presenteert het ontwerp van een FCB en van modulaire bouwstenen (BBs). BvoCs met viskeus vingerpatroon (VFP) zijn gebruikt, waarin menselijke navelstrengader-endotheelcellen (human umbilical vein endothelial cells, HUVECs) zijn gekweekt. Voor zover bekend, is het verbinden van chips met VFP-kanalen met een FCB nog maar één keer eerder ontwikkeld. Daarom was één van de uitdagingen van het project het ontwerpen van de interface tussen chips met VFP kanalen en FCBs. De interface moest zo worden ontworpen, dat bij het verbinden van de BvoCs met een FCB en bij het introduceren van een vloeistofstroom, de integriteit van het VFP-lumen en de cel-lumen gewaarborgd blijft. Stompe naalden zijn als interface methode gebruikt en doormiddel van het verbinden van BvoCs met mini-FCB getest. Met deze interface methode en het aanbrengen van een vloeistofstroom met een afschuifsnelheid van 3.1 Pa blijven de VFP lumen en het grootste deel van de cel-lumen integer. Het gebruik van de ontworpen FCB en de modulaire BBs om continue recirculatie op geparallelliseerde VFP BvoCs te introduceren, kan een waardevolle toevoeging zijn op het onderzoek naar plaque-ontwikkeling en ruptuur. In toekomstige studies kan het toevoegen van vooraf gedefinieerde in- en uitgangen aan de chipvorm de interface tussen BvoCs en FCB verder verbeteren. Daarnaast kan het plaatsen van de chips op een rotator na het zaaien van cellen voor uniformere celaanhechting zorgen. Het geleidelijke verhogen van stroomsnelheden kan voor een betere cel uitlijning zorgen, wat leidt tot uniformere monolagen. Bovendien kan het toevoegen van patiëntmateriaal en meerdere celtypes het onderzoek een stap dichter bij de *in vivo* situatie brengen. Met als gevolg een vermindering van dierproeven, gepersonaliseerde geneeskunde en zorg en een verhoogt aantal goedgekeurde medicijnen op de markt.

Zusammenfassung

Um die Plaque-Entstehung und Plaque-Ruptur zu erforschen, werden Blutgefäße auf einem Chip (blood-vessel-on-chip (BvoCs)) entwickelt. Vorherige Modelle sind daran gescheitert, wesentliche *in vivo* Aspekte wie kontinuierliche Rezirkulation, Parallelisierung, 3D-Gefäßstruktur und physiologische Scherung zu kombinieren. Diese Aspekte sind allerdings erforderlich für das Entwerfen von einem realistischen *In-vitro*-Modell, zum Untersuchen der Plaque-Entstehung und -Ruptur. Ein Hauptgrund für die Behinderung der Forschung von organ-on-chips (OoCs) wie BvoCs ist der Mangel an Standardisierung und Modularität, welche die Einführung von OoCs in die Industrie und Klinik erschweren. Um diese Mängel der OoCs zu überwinden, wurden Fluidik Schaltplatinen (fluidic circuit boards (FCBs)) entwickelt. Ein FCB ist eine modulare mikrofluidische Plattform mit den gleichen Abmessungen wie Zellkulturplatten. Zudem haben FCBs standardisierte Schnittflächen, welche die Integrierung von Komponenten wie Ventilen und Pumpen zusammen mit OoCs in einer Plug-and-play-Weise (Anschließen und Loslegen) ermöglicht.

Diese Masterarbeit präsentiert das Design eines FCBs und Designs modularer Bausteine (BBs). Es wurden BvoCs mit 3D-Lumen mit viskosem Fingermuster (viscous finger patterning (VFP)) verwendet in denen primäre endotheliale Zellen der humanen Nabelschnur (human umbilical vein endothelial cells, HUVECs) kultiviert wurden. Unseren Wissens nach wurde das Verbinden von Chips mit VFP-Kanälen an ein FCB erst einmal getestet. Daher, bestand eine Herausforderung des Projekts darin, die Schnittstelle zwischen Chips mit VFP-Kanälen und FCB so zu entwerfen, dass die Integrität des VFP-Lumens und die Integrität zwischen den Zellen und dem Lumen gewährleistet ist. Um diese Schnittstelle zu testen, wurde ein Mini-FCB entworfen an dessen Einlässe stumpfe Nadeln geklebt wurden. Unter Verwendung dieser Methode und dem Anbringen einer Scherung von 3.1 Pa bleibt das Lumen intakt, allerdings werden die Zellen durch den Flüssigkeitsstrom beinflusst und lösten sich zum Teil ab. Zudem kann die Austauschbarkeit der BBs, resultierend aus dem weiteren Ausbau des Standardisierungsansatzes in der OoC Forschung, Zusammenarbeiten vereinfachen. Die Verwendung des entworfenen FCB und der modularen BBs, um kontinuierliche Rezirkulation auf parallelisierten VFP BvoCs zu ermöglichen, kann eine wertvolle Ergänzung für die Forschung von Plaque-Entwicklung und -Ruptur sein. In zukünftigen Forschungsarbeiten kann das Hinzufügen vordefinierter Einlässe zur Chipform die Schnittfläche zwischen BvoCs und FCB weiter verbessern. Außerdem wird angenommen, dass das schrittweise Erhöhen von Durchflussraten verbesserte Zellausrichtung ermöglicht, welches dazu führt, dass die Zellen in gleichmäßigen Monoschichten wachsen. Darüber hinaus kann das Hinzufügen von mehreren Zelltypen und Patientenmaterial die in vivo Situation besser nachahmen. Dieses kann zur Reduzierung von Tierversuchen führen, personalisierte Medizin ermöglichen und dadurch die Erfolgsraten von Arzneimitteln, die auf den Markt gelangen, steigern.

Table of content

1. List of Abbreviations

2D	Two-dimensional
3D	Three-dimensional
BBs	Building blocks
BvoC	Blood-vessel-on-chips
CVDs	Cardiovascular diseases
ECM	Extracellular matrix
ECs	Endothelial cells
EGM	Endothelial cell growth medium
FCB	Fluidic circuit board
hiPSCs	Human induced pluripotent stem cells
HUVECs	Human umbilical vein endothelial cells
iPSCs	Induced pluripotent stem cells
LTCC	Long-term cell culture
MFBBs	Microfluidic building blocks
mLSI	Microfluidic large-scale integration
NaOH	Sodium hydroxide
OD	Outer diameter
OoC	Organ-on-chip
PDA	Dopamine hydrochloride (polydopamine)
PDMS	Polydimethylsiloxane
PMMA	Polymethylmethacrylate
TOP	Translational organ-on-chip platform
Tris HCl	Tris hydrochloride
VFP	Viscous finger patterning
VSMCs	Vascular smooth muscle cells
WHO	World Health Organization
WSS	Wall shear stress

2. Background

2.1 Plaque development and rupture

According to the World Health Organization (WHO), 32% of all global deaths yearly are caused by cardiovascular diseases (CVDs).[1] Heart attacks and strokes make up 85% of these deaths. Both are mainly caused by a build-up of fats, cholesterol, and other substances on the inner arterial wall (the intima) and can develop into vulnerable plaques prone to rupture (see Figure 1).[1, 4, 5] To study the development of plaques and plaque rupture, animal models have been widely used, but the precise mechanisms involved in plaque vulnerability remain incompletely understood.[5, 8]

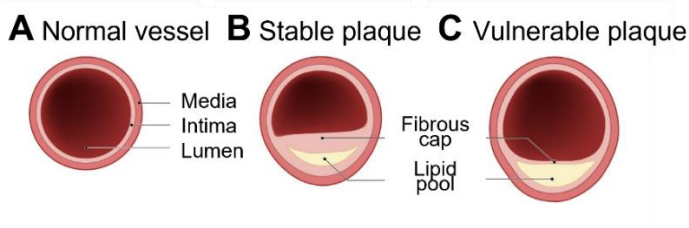

Figure 1: ***Comparison of a normal vessel to vessels with plaque formation.*** *A) A normal vessel with intima and media layer, B) a stable plaque and C) a vulnerable plaque are shown. The vulnerable plaque has a thinner fibrous cap and a higher accumulation of lipids. [5]*

2.2 Shortcomings of common models such as animal models and Organ-on-Chip technology to study plaque development

Mice models have been widely used for pre-clinical drug testing and to study plaque development.[6], [7] Unlike other animal models, mice models are relatively cheap, easy to maintain, and preferred for high-throughput studies.[8] However, unlike in humans, spontaneous plaque rupture does not occur in most mice models and must be induced artificially.[9] Since mice models have limited predictability and reliability regarding drug response in humans, results from animal studies do not always translate into similar results in humans. This is one reason drugs fail the clinical study phase, highlighting the need for a more realistic *in vitro* model**.** [8]

Multiple alternatives to animal models have been investigated to overcome their limitations.[7], [10], [11] Some examples are two-dimensional (2D) cell cultures and other *in vitro* models like three-dimensional (3D) cell cultures in extracellular matrix (ECM) gels (see Figure 2). However, they fail to precisely mimic organ functionalities due to missing microenvironmental factors such as organ-organ interaction. To study CVDs, active perfusion is needed to mimic blood flow, and results must be verified in animal models.[11], [12] A promising *in vitro* technology is **organ-on-chip** (OoC) **technology**.[7], [10]

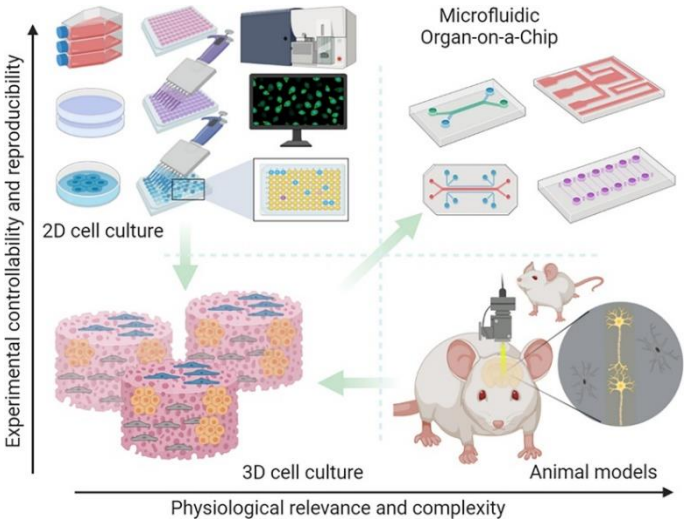

Figure 2: ***A comparison between the physiological relevance and complexity, and the experimental controllability and reproducibility of 2D and 3D cell culture, microfluidic OoCs, and animal models.*** *Where 2D cell culture and microfluidic OoCs both have high experimental controllability and reproducibility, this is low for 3D cell culture and animal models. On the other hand, the physiological relevance and complexity are high for microfluidic OoCs and animal models but low for 2D and 3D cell culture. [7]*

OoC is a microfluidic 3D *in vitro* platform used for disease modelling. OoCs have a physiologically realistic cell culture microenvironment with well-defined geometries and the potential for parallelization and increased throughput.[7], [10] OoCs are used to mimic human organ functions by combining essential aspects of the tissue's surroundings, giving consistent and accurate output.[10], [11] Compared to animal models, real-time visualization and high-resolution quantitative analysis are possible with OoCs.[7], [10], [11] Moreover, cells derived from patients with genetic diseases or several co-morbidities can be integrated, eliminating the disadvantage that co-morbidities cannot be mimicked in animals. OoCs can therefore help improve drug development by more closely replicating the *in vivo* situation.[7], [11] To study plaque development, rupture, and the occlusion of arteries, there is ongoing research about the development of **blood vessel-on-chips** (BvoCs) (see Figure 3). [13]–[15]

2.2.1 Using BvoCs to study plaque development, rupture, and the occlusion of arteries

In the last few years, BvoCs were developed to study thrombosis and plaques. Examples are given by Westein et al. [16], Costa et al. [14], and Cuenca et al.[17], showing that there has been extensive research about BvoCs in the last few years (see Figure 3). Another study used viscous finger patterning, a technique to create 3D vessels on a chip. [18] These studies did make some progress in thrombosis and plaque research. Nevertheless, the combination of the following requirements is still missing but needed to obtain a realistic *in vitro* model: **being in 3D, incorporating multiple cell types, having physiologically relevant flow, and making long-term studies possible**.

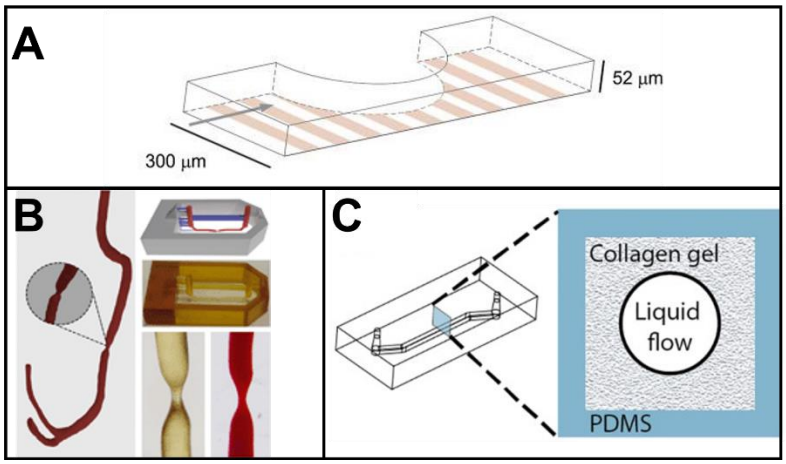

Figure 3: ***Examples of BvoCs.*** *A) A microfluidic stenotic channel designed by Westein et.al.. [16] B) A 3D-printed microfluidic in vitro vascular model designed by Costa et. al.. [14] C) A 3D lumen where several cells were cultured on to mimic the human blood-brain barrier (BBB) on a chip designed by Herland et al.. [18]*

2.2.2 Viscous finger patterning to create collagen-based 3D lumen on BvoCs

During this project, viscous finger patterning (VFP) is used to create collagen-based 3D lumen on microfluidic chips. By seeding ECs in a lumen, a perfusable 3D lumen is created, mimicking the tubular structure of human arteries, reproducing better the shear forces and fluid mechanics in arteries.[15] The technique uses the difference in pressure between fluids having different viscosities. Collagen-1 having a high viscosity, and culture medium having a low viscosity, are used during this project. The high viscosity fluid is introduced into a rectangular channel. When introducing the fluid with low viscosity, it displaces the center of collagen-1 via surface tension-driven pumping. The principle of VFP is shown in Figure 4. [19], [20] To the author's knowledge, before the start of this project, no attempt has been made to implement a chip with VFP channels into a FCB; thus, interfacing the chip and FCB represents one of the project's challenges.

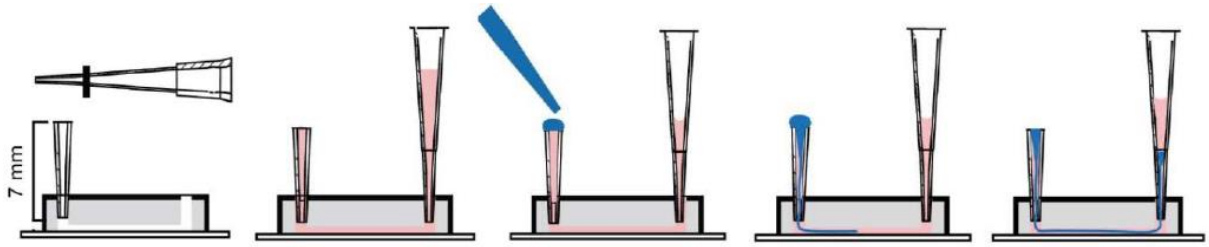

Figure 4: ***VFP principle from left to right.*** *Collagen is indicated in pink and PBS in blue. PBS displaces the center of collagen-1. [15]*

Although OoC technology, like BvoC models, sounds promising, until now, they do not allow for high-throughput studies. There has been some research parallelization and automation of cell cultures on one chip an on introducing flow on a chip instead of having static conditions; however, the combination of all is lacking in the research field of OoC technology. In addition, there is a lack of technical and biological standardization, large-scale manufacturability, and user-friendliness.[21], [22]

2.3 Standardization of OoCs

In the past years, micromechanical valves have been used in OoC research. Integrating those valves on a microfluidic platform enables automated parallelization of different simultaneously performed experiments.[23] However, the lack of standardization in OoC research limits design flexibility. If the microfluidic research field uses standardization, common components like pumps and valves would not need to be reinvented, resulting in shortened development times and cooperation possibilities

between researchers, developers, and end-users, leading to consistent quality and reduced waste.[24], [25] An example is a catalogue of Dekker et al.[24] consisting of products developed according to ISO standards from which researchers can choose and add on. Vollertsen et al.[26] tried to address the challenges mentioned above by designing a chip with multiple valves on a modular and standardized platform. Using this platform, OoCs can be parallelized to perform multiple experiments on different chips simultaneously, allowing for automated medium refreshment.

2.4 Fluidic Circuit Board

A FCB can be seen as a baseplate to which microfluidic building blocks (MFBBs) can be connected.[26] The MFBBs, from now on referred to as building blocks (BBs), and the FCB have standardized dimensions (ISO standards) and the same interface; therefore, the BBs are interchangeable.[24], [26] This allows for combining in-house developed and commercially available products. The BBs are connected via channels in the FCB to form a single, compact microfluidic system, thereby reducing the amount of tubing needed, making the system less bulky, and reducing the chance of leakage.[26], [27] Furthermore, by integrating several OoCs on one FCB, parallelized but also sequential actuation of different biological assays is made possible, increasing the throughput.[26] Also, adding valves to the FCB makes recirculation of fluid between reservoirs possible, reducing bulkiness and the amount of liquid needed.[27] Examples of FCBs have been reported previously.[24]–[29] One example is the Translational organ-on-chip platform (TOP) published by Vollertsen et al.[25] (see Figure 5) describing three FCBs.[26], [27], [30] Up to three BBs per FCB can be integrated into two FCBs. In the third FCB[27] described, recirculation is made possible by the integration of solenoid valves. In addition, in-house developed products are combined with commercially available ones. Recently, de Graaf et al.[29] integrated VFP BvoCs into a FCB. The FCBs have 6-well plate dimensions and can be placed under a microscope. O-rings and Luer locks are used to seal the BBs tightly to the FCB and avoid leakage.[26], [27] FCBs or BBs should be designed according to ISO standards. Having the dimensions and inlet positions the same allows collaboration possibilities.

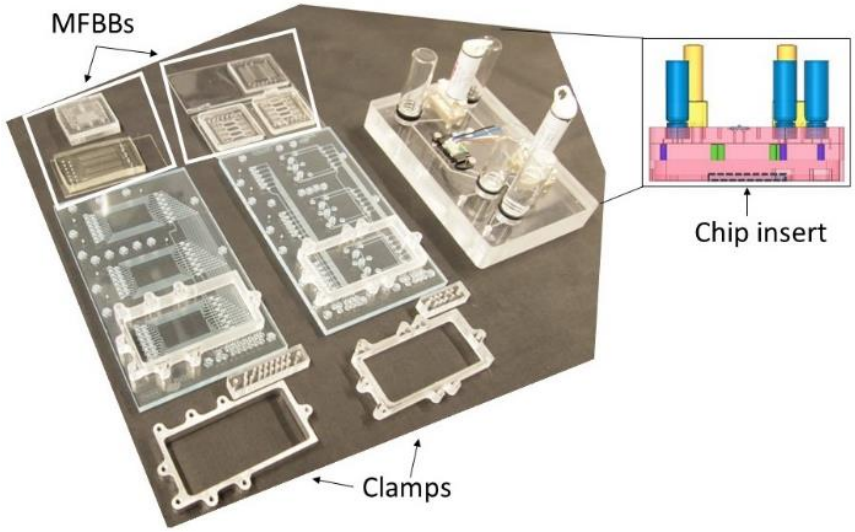

Figure 5: ***Examples of FCBs with well plate format.*** *Up to three BBs can be integrated on the left and middle FCB. Clamps are used to connect the BBs with the FCBs. On the right FCB, in-house and commercially available products are combined, and recirculation of fluid is made possible due to integrated solenoid valves. [25], [27]*

2.4.1 Introducing flow on BvoCs using a FCB

Since in the human body, endothelial cells (ECs) experience unidirectional flow, integrating flow in the study of plaque development and rupture is essential. The cells experience mechanical forces, mainly wall shear stress (WSS) and blood pressure, resulting from the laminar blood flow. They, therefore,

behave differently under flow compared to static conditions. The EC sensibility to WSS is involved in, for example, vascular development processes. It is an essential factor in optimizing blood distribution to tissues and ensuring the proper mechanical function of vessel walls. The WSS found in human arteries is 1-7 Pa.[31], [32]

In a healthy artery, blood flows laminar with secondary flows at places where the artery branches.[33] When this type of flow gets disturbed, the laminar flow turns into turbulent flow.[34] The Reynolds number describes both types of flow and is about 2000 for blood flow, which is classified as laminar flow. A change in the geometry of the artery, blood viscosity, or flow velocity can alter the flow pattern. An example would be the alteration of blood flow by atherosclerotic plaques narrowing the artery, showing the importance of integrating continuous flow into BvoCs, allowing the study of the influence of shear stress.[33], [36] De Graaf et al.[29], Vivas et al.[27] and Vollertsen et al.[25] introduced flow on OoCs using FCBs.

2.5 Aim of the study

Although there has been extensive research in the area of BvoC technology, important features to establish a realistic *in vitro* model for CVD studies are still lacking. Until now, no platform exists that combines **continuous reperfusion** on **parallelized 3D VFP BvoCs** with **physiological shear**. Therefore, this thesis aims to

1) Make designs of a **FCB and BBs that can combine the aforementioned requirements. Integrating BvoCs into this platform increases the likelihood of making long-term cell culture (LTCC) possible** by establishing a more *in vivo*-like model, providing more insights into plaque development and rupture.
2) Test the central, modular building block, particularly with a **focus on the combination of FCB technology with the VFP method**

2.6 Thesis outlook

The design of the FCB and the modular BBs are described. Decisions for certain pump and valve types were made keeping the requirements a good BvoC model has to meet in mind. To test the interface between the FCB and the BvoCs, a mini-FCB was designed and tested. Fluid flow experiments were performed to examine the influence of flow on the integrity between VFP lumen and BvoC-channels and the cell integrity in VFP lumen.

3. Design of the fluidic circuit board with modular building blocks

This chapter introduces the suggested FCB design and describes the design choices and techniques used. The design is based on the requirements defined to make BvoC models a more realistic *in vitro* platform to study plaque development.

3.1 Design requirements

Before proposing the FCB design, the following design requirements were defined:

1. **Continuous flow**: By introducing continuous flow on BvoCs, cellular responses to physical forces resulting from fluid flow can be assessed. The *in vivo* situation is more accurately reproduced.
2. **Reperfusion**: Molecules such as tissue factors pass cells in the arteries more than once. Integrating fluid reperfusion will result in a more realistic *in vitro* model.
3. **Parallelization**: Higher throughput is possible when executing experiments parallel to each other.
4. **3D (VFP) lumen**: Round 3D lumen more closely resemble the *in vivo* situation in terms of fluid mechanics. Shear forces in lumens are spread more realistically than in rectangular channels.[57]
5. **Physiological shear**: Shear influences cell behavior. When having physiological shear, the cells are expected to behave more like *in vivo*. The WSS in human arteries lies between 1-7 Pa.[31], [32]
6. **Long-term cell culture (LTCC)**: Plaques develop over time. Being able to execute cell culture experiments over a longer period will help to model the *in vivo* situation better.

3.2 FCB and modular BBs

The FCB is based on designs of Vivas et al.[27], Vollertsen et al.[25], and Dekker et al.[24]. De Graaf et al.[29] integrated VFP BvoCs into an FCB. However, this work was published after the experimental phase of this study was completed. Therefore, the design presented in this study is not based on the FCB design of de Graaf et al.. The total size of the FCB design depicted in Figure 6 has a footprint of 12,75 cm (l) x 8,25 cm (w), which corresponds with the standard dimensions of a 6-well plate and assures compatibility with microscope stage inserts allowing easy analysis.[27] The size of the different BBs and the in- and outlet layout and dimensions are designed according to standard-defined ISO values (ISO22916), allowing interchangeability with other BBs. The separate BBs are indicated in the FCB design by intermittent lines and will be designed separately from the FCB. In this FCB design, only BB 3, the flow sensor, is a commercially available BB. All other BBs will be developed in-house. The four BBs are connected via channels inside the FCB and numbered from left to right.

In this FCB design, push-up valves are integrated and can be used for the automation and continuous recirculation of fluid. Peristaltic pumps, consisting of three push-up valves, allow for continuous flow. The FCB can be controlled manually or automatically by using customized programs such as LabVIEW. The program allows for automatic medium refreshment and imaging. The design of the BvoC has already been developed prior to this project and does not have ISO standards. To use the FCB for chip designs other than the BvoC, BB 4 has to be redesigned.

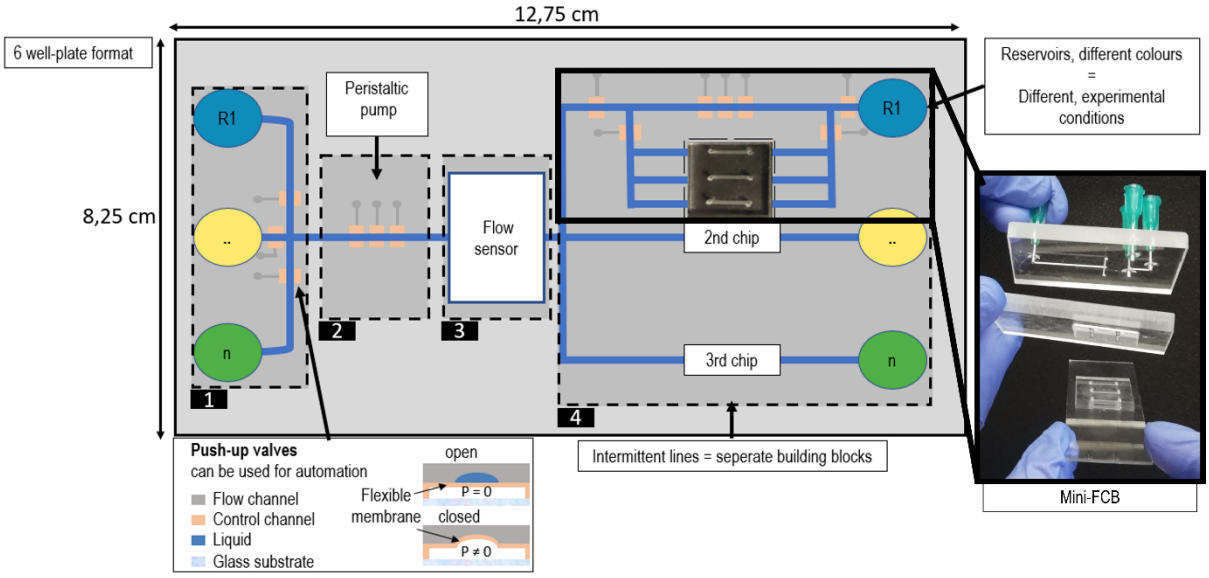

Figure 6: ***Design of the FCB.*** *Schematic Illustration of the top view of the FCB design and on the right side an image of the mini-FCB.*

The BBs will be connected in a plug-and-play fashion by inserting them from above into the FCB. Up to three BvoCs, each consisting of three channels, can be connected to BB 4 from below via blunt needles. By inserting the chips from below, imaging is made easier since the optical path is shorter. The interface between the BvoCs and FCB will be similar to the BvoC and mini-FCB interface, which is explained in more detail in the Mini-FCB section. The reservoirs are tanks having caps and a Luer lock interface (see Appendix Figure 14) and can be placed from above in BB 1 and BB 4. Since the BBs are made from PDMS, PDMS will seal the space between reservoir and inlet.

Each reservoir in BB 1 can have a different experimental condition. Moreover, the pump in BB 2 can mix conditions, e.g., one part of reservoir 1 can be mixed with ten parts of reservoir 2 and directed into the top chip by opening and closing the respective valves. The flow sensor measures the flow rate with which the chip is filled. Next, the second and third chip can be filled with the desired condition in the same way. When having three different conditions in each reservoir, three additional conditions can be obtained by mixing the fluids using the peristaltic pump in BB 2. Since the chips are filled one after the other, each chip can be filled with a different flow rate. The recirculation compartment of BB 4 is explained in more detail below.

Overview of the BBs and their functions:

1. BB1
    - A BB with **reservoirs** and **valves**. Each reservoir can be used for a **different condition** and can be **addressed separately** by actuating the **specific valve**. (see requirement 2 and 3)
2. BB2
    - The BB consists of three valves that form a **peristaltic pump**. The peristaltic pump is integrated into the design **to mix** and **distribute** the liquid. (see requirement 1 and 2)
3. BB3
    - A BB with a **flow sensor**. The flow sensor **measures** the **flow velocity** when the chips are filled with fluid. (see requirement 5)

4. BB4
    - A BB with **recirculation compartment and chip insertions for three VFP BvoCs** to allow for **parallelization and continuous flow.** Each chip consists of three channels and is connected to its own reservoir, enabling simultaneous testing of up to three different experimental conditions (indicated by the different colors). (see requirement 1, 2, 3, 4, and 5)
5. Mini-FCB
    - The mini-FCB is designed to **test the interface** between the VFP BvoCs and the FCB (see Figure 6).

3.3 Push-up valves for fluid routing

Even though it is easy to generate liquid flow, controlling flow is challenging. Therefore, to direct and control fluid flow, valves can be integrated into a microfluidic chip. The types of valves discussed in this thesis are solenoid, check valves, and pneumatic Quake valves, as these valves were used in earlier FCB designs (see Appendix Table 3).[24]–[27]

Solenoid valves, for example, were used by Vivas et al.[27] and check valves by De Graaf et al.[29]. However, since both are bulky, Quake valves are used for this FCB design.[27] Quake valves[23] are pneumatic valves easily integrated into soft lithography designs. They reduce bulkiness and costs of the FCB design. Quake valves can be divided into push-up and push-down valves (see Figure 7). Since push-up valves, compared to push-down valves, have the advantage of requiring lower actuation pressures and allowing for the design of taller flow channels, they are used for the FCB design. Push-up valves consist of a semi-circular flow channel located perpendicular to a control channel. The channels are separated by a membrane. The membrane bends upwards and closes off the flow channel when pressurizing the control channel.[23] In Quake valves, the dead-ended control channel is filled with water to prevent air from penetrating the membrane. The channels can be regulated using independent pressure lines controlling the fluid flow.[26] The pressure needed to close the flow channel is determined by the membrane stiffness and the valve dimensions. The flow channel´s height should not be too high to avoid extended closure times of the valve, which affects the flow rate, but high enough so cells can pass. [21], [26]

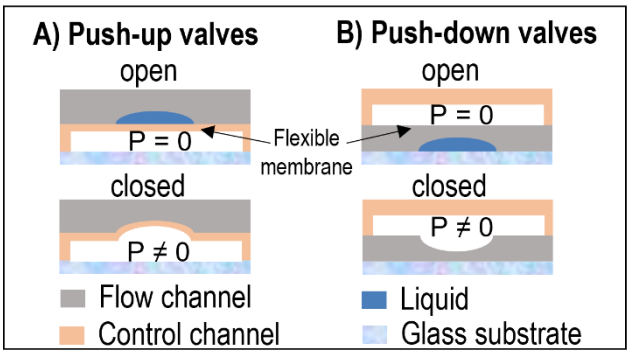

*Figure 7: **Schematic illustration of push-up and push-down valves.** The flexible membrane situated between the two channels is deflected when applying pressure to the control channel (P ≠ 0), and the flow channel is closed. A) Push-up valves: the membrane, incorporated in the control channel, bends upwards when pressurizing the control channel (P ≠ 0), blocking the flow channel. B) Push-down valves: the membrane, incorporated in the flow layer, bends downwards when the control channel is pressurized (P ≠ 0), blocking the flow channel.*

BB 1, 2, and 4 contain push-up valves. By opening and closing certain valves in BB 1, the desired condition can be accessed. Next, the peristaltic pump in BB 2, consisting of three valves in a row, mixes and distributes this condition to a BvoC. The opening and closing of the valves in BB 4 determine which

chips are filled with fluid. For example, if the top valve in BB 1 and the valves in BB 4 connected to chip 1 are open, condition 1 can be pumped into the top chip (see Figure 6 and paragraph 3.6).

3.4 Peristaltic pumps for the introduction of continuous flow

Pumps allow the introduction of flow and circulation of fluid in a microfluidic chip. Various types of pumps are used in microfluidic research, including syringe pumps, pressure pumps, and peristaltic pumps (see Appendix Table 4).[21], [38], [39] However, off-chip pumps, like syringe and pressure pumps, are limited by their parallelization possibilities, increased bulkiness, and costs.[40], [41]

When considering pumps for FCBs, flow rates, and flow patterns must be considered next to bulkiness and costs, as in arteries, ECs are exposed to pulsatile flow. Peristaltic pumps generate pulsatile flow and are hence integrated into the FCB design.[42], [43] Additionally, integrating peristaltic polydimethylsiloxane (PDMS) pumps on the FCB results in one device allowing fluid flow control without requiring accurate regulation of off-chip pressure sources, minimizing external fluidic and electronic connections.[23], [44] Bossink et al.[21] integrated on-chip peristaltic PDMS pumps on a chip, from now on referred to as Bossink pumps. The channel dimensions of the pumps used are 1000 µm x 400 µm (width x length) and can reach flow rates of up to 48 µl/min (shear stress 0.37 Pa), which is higher than the flow rates of 0.15 µl/min that classic on-chip peristaltic pumps can generate. [45]–[49] Furthermore, instead of photolithography, micro-milling is used to create moulds for valves, requiring fewer time-consuming fabrication steps and allowing for more design flexibility. The Bossink pumps can achieve pulsating flow by having three valves in series, which can be sequentially actuated. The pumping principle is depicted in Figure 8, where an open valve is indicated with 1 and a closed valve with 0. The valves are actuated one after the other in a 6-phase pattern, pushing fluid forward.[40], [50]

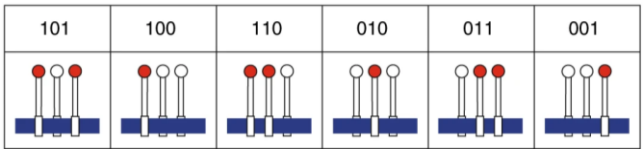

Figure 8: ***Pumping principle of the Bossink pump with a 6-phase actuation pattern.****[30] Open valves are indicated in red and with a 1 and closed valves with white and a 0.*

There is one peristaltic pump in BB 2 and three in BB 4. The peristaltic pump in BB 2 is used to mix and distribute fluid. In BB 4, each recirculation compartment has its own peristaltic pump, allowing continuous flow on the BvoCs. Each chip must have a pump to keep the different conditions of each chip separated. The advantage of having one pump per chip is the usage of different flow rates per chip, allowing one to examine the effect of different shear stresses.

3.5 Mini-FCB design

One of the challenges of this project was to connect VFP BvoCs to a FCB without destroying the VFP lumen. The mini-FCB is designed to test the interface between the BvoC and the FCB, located in BB 4, and to examine whether the VFP lumen remains intact when introducing flow. The design of the mini-FCB consists of a top and a bottom part micro-milled in Polymethylmethacrylate (PMMA) plates (see Figure 9). The top part of the mini-FCB mimics the channels in BB 4 leading to the chip insert. The bottom part is designed to test the connection of the chip to the FCB using a chip pocket. Figure 9 shows that the two parts of the mini-FCB are connected by aligning the inlets. The chip is inserted from below, resulting in a shorter optical path between the microscope and the chips, making imaging easier.

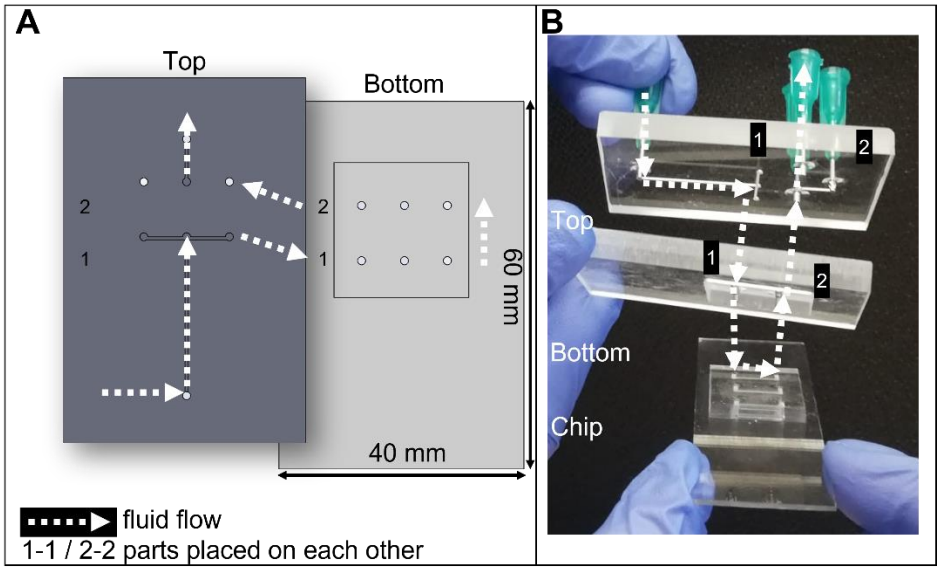

*Figure 9: **Top and bottom part of the mini-FCB** A) as SolidWorks design and B) micro-milled. The fluid pathway is shown with white arrows. Correct placement of the two plates by matching number 1 and 2 of each plate.*

The mini-FCB is not designed according to ISO values (ISO22916), as it will not be used in the final design. In the final design, the interface is in BB 4. Since the chip was designed prior to this project, the distance between the inlets is not designed according to the ISO values; thus, the chip pocket does not have ISO values. The top and bottom plates have a length of 60 mm and a width of 40 mm. The inlets of both parts have a diameter of 1.30 mm. The channel width is 0.50 mm. The chip insert is 22 mm by 22 mm. The inlets of the chip pocket are on the x-axis, 7 mm apart from each other, and 9 mm on the y-axis.

3.5.1 Adjustments of the mini-FCB design

Some optimization steps were performed before the final mini-FCB design was used for fluid flow experiments. The initial design of the top part (see Appendix Figure 15) was adjusted to ensure that the liquid travels the same distance for all three channels. In the first design (see Appendix Figure 15A), the fluid in the two outer channels traveled a longer distance (L2 = 7mm) compared to the fluid in the middle channel. Therefore, the outlet of the middle channel was shifted up by the same distance (L2) (see Appendix Figure 15B). Having all parameters included in the formula to calculate the resistance of a cylindrical vessel the same, results in equal flow distribution since the hydraulic resistance R is the same for each channel:

$$R = \frac{8\,L\,n}{\pi r^4} \qquad (1)$$

where r = vessel radius, L = vessel length, n = viscosity.[51]

3.5.2 Interfacing BvoCs with the mini-FCB

This project´s challenge was to interface the BvoCs and the FCB. A mini-FCB was designed and used to test this interface. The BvoCs have VFP channels that must remain intact when connecting the chips to the FCB. Moreover, when introducing flow, the connection must be leak-free.

To the best of our knowledge, only one attempt has been made to integrate a chip with VFP channels into a FCB.[29] This study uses Luer locks to connect VFP BvoCs to the FCB. In other studies, glass capillaries[52] and O-rings[25], [26] were used to interface OoCs with the FCB. However, in these studies, the OoCs did not have VFP channels. Nevertheless, these methods were compared as possible interfacing methods. Compared to the other methods, using glass capillaries is time-consuming as it

requires several fabrication steps and waiting steps. Because O-rings are placed on top of the inlets and touch the PDMS, the VFP lumen may be destroyed. Therefore, either Luer locks or blunt needles can be used to touch the PDMS as little as possible. However, the SolidWorks design required for Luer lock inlets is slightly more complex than designing straight holes as needed for blunt needles. Therefore, blunt needles are used in this first mini-FCB design. To connect the chip with the mini-FCB, blunt needles are glued to the inlets of the upper part, and only the steel needles are glued to the inlets of the chip pocket. The BvoCs are pushed onto the blunt needles (see Figure 9).

3.6 Unidirectional recirculation of fluid and partially refreshing

Figure 10 shows how unidirectional recirculation of fluid and partial refreshing is visualized with BB 4 on the proposed FCB design. The design is based on the recirculation chip of Bossink et al.[40]. Continuous recirculation on the BvoC is achieved by closing valve 2 and actuating the peristaltic pumps. Partial liquid refreshment can be performed by isolating the chip from the liquid supply by closing valves 3 and 4 and opening valve 2. Only in the upper channel liquid is replaced.

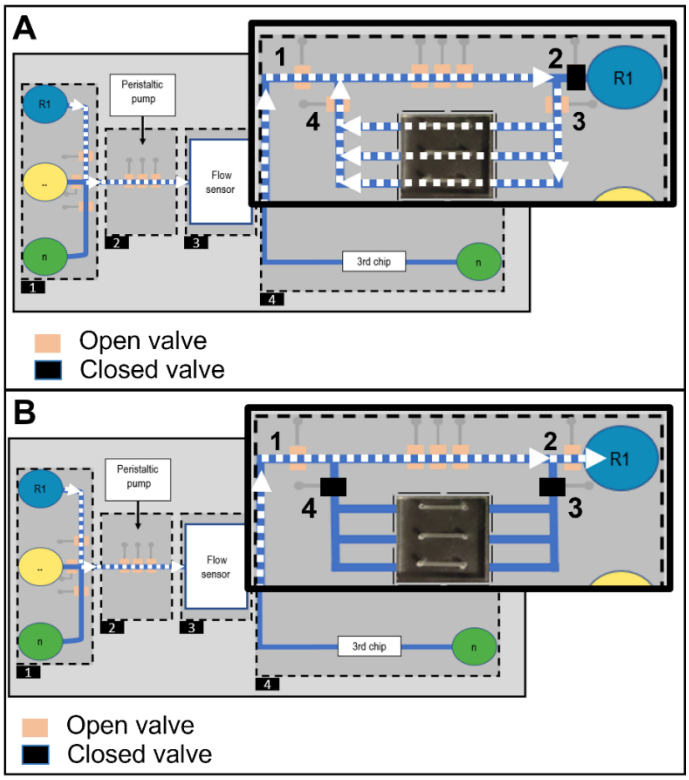

Figure 10: ***Close-up of the fluid recirculation unit of BB 4.*** *The valves are indicated with numbers, and the fluid flow with arrows. A) Valve 1, 3, and 4 are open. Valve 2 is closed. Recirculation of fluid using the peristaltic pump is indicated by the arrows. B) Valves 3 and 4 are closed, allowing fluid to flow from the upper channel into the reservoir. Liquid refreshment is performed.*

3.7 Long-term cell culture

Combining the mentioned requirements of introducing continuous recirculation on a 3D VFP BvoC with physiological flow on a FCB is expected to enable long-term cell culture (LTCC). The current implementation time of the experiments using VFP BvoCs achieved by this research group (BIOS) is five days. To place this into context, Apo E knockout mice, used in atherosclerosis research, are kept alive for 14 to 22 weeks.[53], [54] The research group of Cuenca et al. [17], which studied engineered 3D vessels-on-chip, was able to perform cell culture for up to 21 days by combining human induced pluripotent stem cells (hiPSCs)-derived endothelial- (EC) and vascular smooth muscle cells (VSMCs). This study states that adding VSMCs to hiPSC-EC promotes self-organization and vessel stability. Next,

their results indicate that the most essential steps of vasculogenesis and remodeling of the blood vessel network occurred in the first 7 days of VoC culture. However, they do not introduce physiological flow but gravity-driven flow. During this project, only one cell type (HUVECs) is used, which could lead to reduced vessel stability[55] compared to the 3D vessel-on-chip used by Cuenca et al.[17], as literature states that the addition of VSMCs increases vessel stability [17], [55]. Pediaditakis et al.[56] was able to perform cell culture for up to 8 days using continuous flow but no physiological flow. In this study, after 2 days of static culture, fluid flow of 60 µl/h was introduced. Herland et al.[18] kept their cells in culture for 5 days, but not under continuous flow. This project aims to keep the cells in culture for at least 8 days as this is the state-of-the-art in current blood vessel studies applying continuous flow and using only one cell type.[56]

Table of requirements for a realistic BvoC model comparing the current model and the proposed FCB model

Table 1 provides an overview of the requirements to bring the BvoC model towards a more realistic *in vitro* model to study plaque development and rupture. The definitions of the requirements are given. It is shown how the requirements are met in the model currently used by this research group (column 3, state-of-the-art: VFP BvoC model) and how the FCB design meets them, showing the improvements made by integrating the BvoC model into the proposed FCB design.

Table 1: ***Overview of the requirements for a realistic BvoC model.*** *The current model is compared to the proposed BvoC model.*

Requirements	**Definition**	**State-of-the-art**		**BvoCs on a FCB**
		VFP BvoC model	**FCB**	**Proposed design**
3D	Round, collagen lumen	VFP	VFP [29]	VFP
Continuous flow		Rocking Plate	Pressure pump [27]	Peristaltic PDMS pump [21]
***In vivo* shear stress**	1-7 Pa [31]	Pipet	Pressure pump [27]	Peristaltic PDMS pump [21]
Recirculation of fluid	Unidirectional	Static	Solenoid and push-up valves [27]	Push-up valves
Parallelization	Integrating multiple chips on one platform [25]	1 chip with 3 channels	12 VFP channels on one FCB [29]	3 chips with each 3 channels
Long-term cell culture	8 days [56]	5 days	5 days [27]	By integrating new features – getting closer to in vivo
Multiple cell types	HUVECs and VSMCs [17]	1 cell type (HUVECs)	Not yet tested with FCB	Future experiments

4. Materials & Methods

4.1 Fabrication of the mini-FCB

The mini-FCB, consisting of a top and a bottom part, was designed in a CAD design software (SolidWorks®, version 2021, Dassault Systémes, France) and translated to compatible files using Autodesk HSM software. The top and bottom part of the mini-FCB were micro-milled one time from 5.8 mm and one time from 7.5 mm thick polymethylmethacrylate (PMMA, Arkema innovative chemistry) using a milling machine (Datron, Mühltal, Germany). Micro-milling selectively removes material in the X, Y, and Z-direction using rotating cutting tools like mills and drills. Double-fluted end mills with a flute diameter of 0.4 mm, 2 mm, and 5 mm and drills with a diameter of 1.0 mm, 1.2 mm, and 1.3 mm (Datron, Mühltal, Germany) were used for milling.

Blunt needles (TE series dispensing needle, METCAL, Cypress, California) were attached to the PMMA plates. Before attaching blunt needles to the bottom part, the plastic needle hub was removed from the steel tubing. Different diameter blunt needles were used for the different dimensions of the inlets (see Table 5). The needles used had an outer diameter (OD) of 0.81 mm, 0.91 mm, and 1.27 mm. For the top part, blunt needles with an OD of 1.27 mm were used. From the table, it can be seen which needles were glued and which were hammered to the inlets. Two different adhesives were tested; epoxy adhesive (Loctite Hysol EA M-31CL, Henkel, Düsseldorf, Germany) and UV curable adhesive (Norland Optical Adhesive 81, New Jersey, United States). To cure the epoxy adhesive, the PMMA parts were placed overnight in an oven at 60°C. UV light with 400 MW/cm^2 was used five times for 10 seconds to cure the UV-curable adhesive.

To bind the two parts of the mini-FCB, solvent bonding and adhesive bonding were considered. Solvent bonding requires chemicals and multiple fabrication steps, resulting in a more time-consuming fabrication.[27] Using double sided adhesive tape, the tape is placed between the two PMMA parts making it an easy and fast fabrication method.[57], [58] Therefore, it was chosen to perform the multi-layered fabrication of the mini-FCB through adhesive bonding. Prior to placing the double-sided adhesive tape (AR care 90106NB, Adhesive Research®, Glen Rock, Pennsylvania) between the two parts of the mini-FCB, holes had been placed at the places of channels and inlets to avoid covering them. This was done using a plotter (Cricut Maker™ machine, United States).

4.2 Testing fluid flow

Prior to bonding, fluid accessibility of the chip via the bottom part was tested by attaching the chip (see Chip fabrication) to the chip pocket and pushing food coloring through using a 1.1 mm x 40 mm needle (BD MicrolanceTM 3, Ireland) connected to a 10 ml syringe (Injekt® Solo, B|Braun, Germany). Next, the top and bottom part were bonded together. The chip was inserted into the mini-FCB. Food color was pushed through using tubing with an inner diameter of 0.8 (TYGON, France) connected to a syringe. Thereafter, the mini-FCB was connected to a syringe pump (Harvard apparatus PHD 2000, Hollisten, Massachusetts), and food color was pushed through. Next, chips with VFP channels (see viscous finger patterning protocol) were inserted into the mini-FCB and connected to the syringe pump. VFP chips seeded with Human umbilical vein endothelial cells (HUVECs) (Pooled Donor C2519A, Lonza, Basel. Switzerland) (see cell culture protocol) inserted in the mini-FCB were connected to a syringe pump. Pictures of the fluid flow experiments using a syringe pump were taken before and after with an EVOS M5000 microscope (4x, Thermo Fisher Scientific, Waltham, MA, USA). The fluid flow was monitored on a Leica DM IRM (4x, Leica, Wetzlar, Germany) using a microscope software platform (LASV4.10, Leica, Wetzlar, Germany). For all experiments performed with the syringe pump a flow rate of 400 µl/min was used (shear stress of 3.1 Pa, see Appendix for calculations).

4.3 Chip fabrication

4.3.1 PDMS soft lithography

Conventional PDMS-based soft lithography was performed to fabricate the chips. A negative PMMA mould was used. The dimensions of the channels were 10 mm x 0.5 mm x 0.5 mm (LxWxH). PDMS (Sylgard 184 Silicone elastomer kit, Dow corning, Michigan, USA) was mixed (1:10 (%w/w) base:crosslinker ratio) and degassed for 1h. PDMS was poured on the mould and spin-coated on glass slides for 5 sec at 500 RPM and 30 sec at 1500 RPM. The chip mould and the glass slides were left to cure overnight at 60°C. PDMS was removed from the chip mould, and the chips were cut. Inlets were punched using a 1mm biopsy punch. After punching, dust was removed using Scotch tape. The surfaces of the mould and the glass slides were activated by exposer to air plasma (50W) for 6 min. Hydroxyl groups are formed on the PDMS surface, allowing surface functionalization. Next, dopamine hydrochloride (PDA) (H8502-5G, Sigma Aldrich, Missouri, United States) coating was performed. PDA functionalizes the PDMS surface to achieve a better binding of collagen-1 to the chip. During the preparation of the PDA solution of 1mg/ml tris hydrochloride (Tris HCl) (10mM Tris-HCl, pH 8.5; Tris base, Sigma Aldrich, 37% HCl, Merck), the bonded chips were kept in an oven at 60°C. Then, PDA was added to each channel, and the chips were incubated at room temperature for 1h-1.5h after which it was washed with MilliQ and dried using an aspirator (Vacusafe comfort, IBS Integra biosciences, Shanghai, China). The chips were either immediately used for VFP or stored for up to 14 days.

4.3.2 Viscous finger patterning

To create a 3D collagen lumen and allow cell attachment, viscous finger patterning (VFP) was performed on the chips. A high concentration rat tail derived collagen-1 (either 9.90 mg/ml, Corning, New York, United States or 10 mg/ml, ibidi, Fitchburg, Wisconsin) mixture was prepared according to a protocol optimized by de Graaf et. al..[15] The final solution had a pH between 7.0 and 7.2 and a concentration of 5 mg/ml. Depending on the concentration of collagen-1 used, either 5.81 µL or 5.75 µl of Sodium hydroxide (NaOH) (1M, S8045-500G, Sigma-Aldrich, Missouri, United States) was added together with 50 µl 10x PBS + phenol red and either 191.66 µl or 194.25 µl dH2O. Next, 252.53 µl or 250 µl collagen-1 was carefully added to avoid air bubble formation. The collagen-1 mixture was vortexed and spun down to remove air bubbles. All reagents were kept on ice during the preparation. The pH change, resulting from the addition of NaOH, and the temperature change allow crosslinking of the mixture and the formation of the gel.

Before preparing the mixture, 7 mm cut pipette tips were placed into one inlet of each channel. The chips were stored in an incubator at 37°C until the mixture was ready to use. 10µl of collagen mixture was added with ice-cold pipette tips to the channels until a meniscus formed on top of the 7 mm pipette tip on the other inlet. The pipette tip was left in the inlet, and 2.2 µl cold PBS was added on top of the collagen meniscus. The chips were incubated for 60 min. After incubation, endothelial cell growth medium (EGM, Cell Applications, California, United States) was added to the channels by replacing both pipet tips with new pipet tips filled with medium. Lumen formation was analysed under the microscope (4x, brightfield, EVOS). The chips were placed in an incubator overnight at 37°C. After refreshing the medium in the channels using gel-loader tips, cell seeding was performed. A schematic drawing of the VFP principle is shown in Figure 4.

4.3.3 Cell culture

HUVECs were cultured in endothelial growth medium (EGM, Cell Applications, California, United States) in a collagen I-coated T-75 flask (CELLCOAT®, Greinder Bio-One, Kremsmünster, Austria) at 37°C and 5% CO_2 humidified incubator. After reaching 80% confluency, the cells were washed with 10 ml of Dulbecco's phosphate-buffered saline DPBS 1x (14190-094, gibco, Massachusetts, United States). PBS was removed, and 3 ml trypsin-EDTA 1x (15400-054, gibco, Massachusetts, United States) was added

and incubated for 2-2.5 min at 37°C. By adding 7 ml of EGM, trypsin activity was stopped. The cells were centrifuged at 390g for 5 min (AllegraTM X-12R Centrifuge, Beckman Coulter, California, United States), whereafter, the supernatant was removed from the cells. The cells were resuspended in EGM. The volume of EGM added to the cell pellet corresponds with the minimum volume needed to fill all channels. The volume was calculated prior to cell seeding and depended on the amount of chips used. The cell concentration was calculated using an automated cell counter (Luna™ Automated Cell Counter, Westburg, Utrecht, The Netherlands). The cells were resuspended in EGM to a concentration of 5*10^6 cells/ml. 10 µl cell solution was added with a gel loader tip (greiner bio-one, Kremsmünster, Austria) to each channel of the chip. To ensure cell attachment to the top of the channel, the chips were inverted after adding cells to the channel for at least 30 min. Seeding the cells twice ensures the entire cell covering of the lumen. After 30 min of incubation, 200 µl medium was added to the cells. The cells were cultured for 48h, during which the medium was changed twice. Cells with passage number 9 were used for seeding in the chip.

5. Results

This chapter describes and discusses the experiments executed during this thesis. The results can be divided into three topics: the design of the FCB, which is discussed in the design chapter, the fabrication of the mini-FCB, and the testing of the interface between the BvoCs and the mini-FCB.

Fabrication and testing of the Mini-FCB

The mini-FCB is designed to test the interface between the VFP BvoCs and the FCB. The challenge was to keep the VFP lumen intact when interfacing with the mini-FCB and when introducing fluid flow.

5.1 Interfacing BvoCs with the mini-FCB

After micro-milling the top and bottom parts of the mini-FCB, blunt needles with an OD of 1.27 mm were glued to the inlets (see Figure 11). Blunt needles should allow for a leak-free interface between the tubing and the chip to the mini-FCB. While curing the epoxy adhesive, the needles penetrated the in- and outlets and protruded from the other side (see Appendix Figure 16). Therefore, the diameters of the in- and outlets of both parts were changed; the first design went from 1.3 mm to 1.2 mm, and the second design from 1.3 mm to 1.0 mm. Needles with an OD of 0.81 mm and 1.27 mm were used. Applying UV curable glue instead of epoxy adhesive accelerated the curing time. Simultaneously, it was tested whether hammering would be more efficient and prevent the needles from sticking out on the other side. During fabrication, it was observed that hammering induces cracks in the PMMA. Using glue and placing the parts on a flat surface during curing ensured that the needles did not penetrate and no cracks were induced. Blunt needles were glued to the top part (Figure 11, B, and C), and blunt needles where the plastic part was removed were glued to the bottom part (Figure 11, E, and F).

5.2 Testing fluid flow through chips with the bottom part of the mini-FCB

Next, it was tested whether fluid could go through the chips when having the chips attached to the chip pocket via the blunt needles (OD of 0.81 mm and 1.27 mm). This experiment was performed to test whether addressing chips with fluid is possible when using blunt needles for the interface between the chips and the mini-FCB. The chips were attached to the bottom part of the mini-FCB, and food color was pushed through using a syringe. It was observed that needles with a small OD (0.81 mm) attached to the mini-FCB were deformed (see Appendix Figure 17). The chips were not addressable with fluid. The deformation resulted from removing the plastic hub from the steel needle. Using needles with an OD of 1.27 mm, the needles deformed less, and chips were addressable with liquid, as evidenced by fluid flowing from one inlet to the other (see Appendix Figure 18). The remaining experiments were performed with blunt needles with an OD of 1.27 mm attached to inlets with a diameter of 1.3 mm.

5.3 Multi-layered fabrication of the mini-FCB and testing of the bonding efficiency

The top and bottom parts of the mini-FCB were bonded by adhesive bonding, and the BvoC was inserted into the chip pocket from below (see Figure 11). Before bonding, holes were cut in the adhesive tape to avoid covering the channels and inlets.

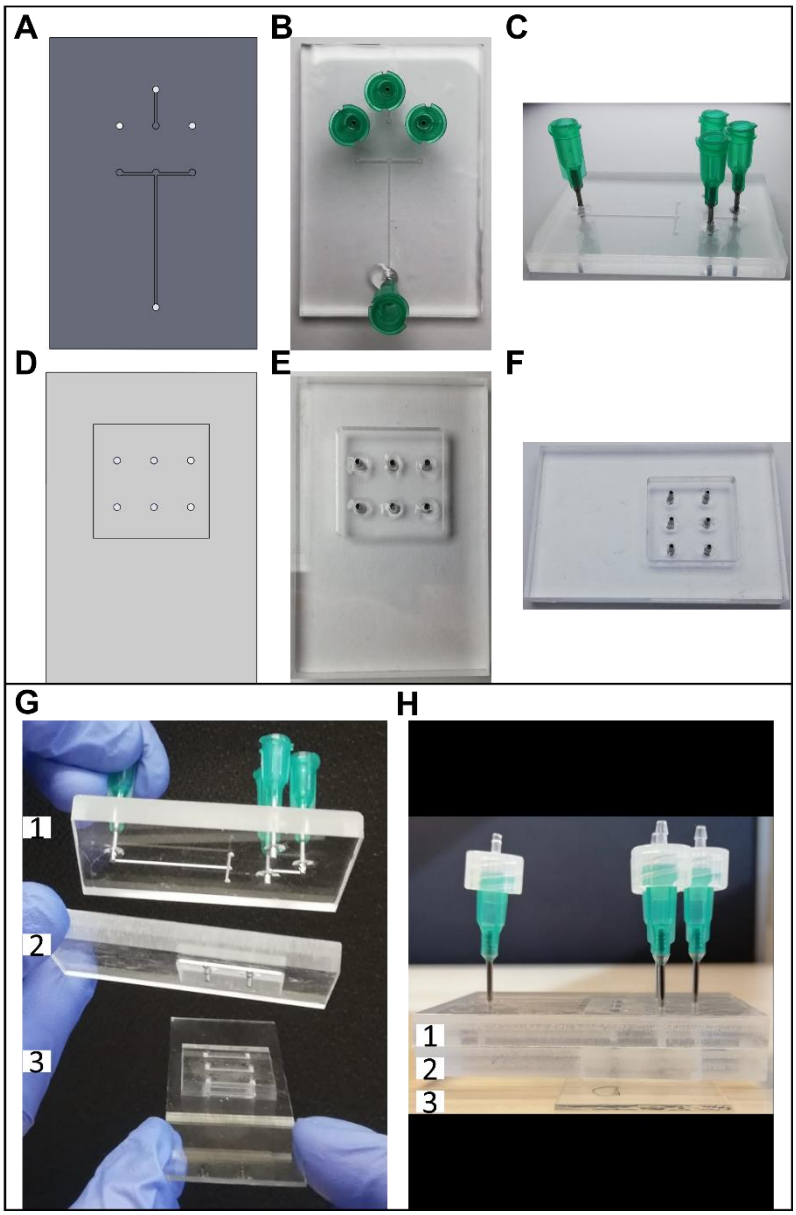

Figure 11: ***Designs of the top and bottom parts of the mini-FCB and the multi-layered fabrication.*** *Top and bottom parts of the mini-FCB as SolidWorks designs (A and D, respectively) and the micro-milled PMMA parts (top part B and C, bottom part E and F). Blunt needles were attached to the top part (B and C), and blunt needles without plastic hub to the bottom part (E and F). G) Alignment of top and bottom part and insertion of the BvoC into the chip pocket. H) mini-FCB after adhesive bonding. 1: top part, 2: bottom part, 3: BvoC*

Food color was pushed through the mini-FCB using a syringe. During the first experiment, air bubbles were observed in the adhesive tape. Repeated fabrication of adhesive bonding resulted in fewer bubbles in the adhesive tape. Performing the experiment with a mini-FCB with needles glued to the inlets, leakage was only observed where the tape was cut for the channels and inlets, as indicated in Figure 12. In addition, it was observed that after the channels had been pre-wetted, all three channels of the chips filled evenly with liquid. Whether all three channels filled simultaneously when using a pump was not determined systematically and must be investigated in future research.

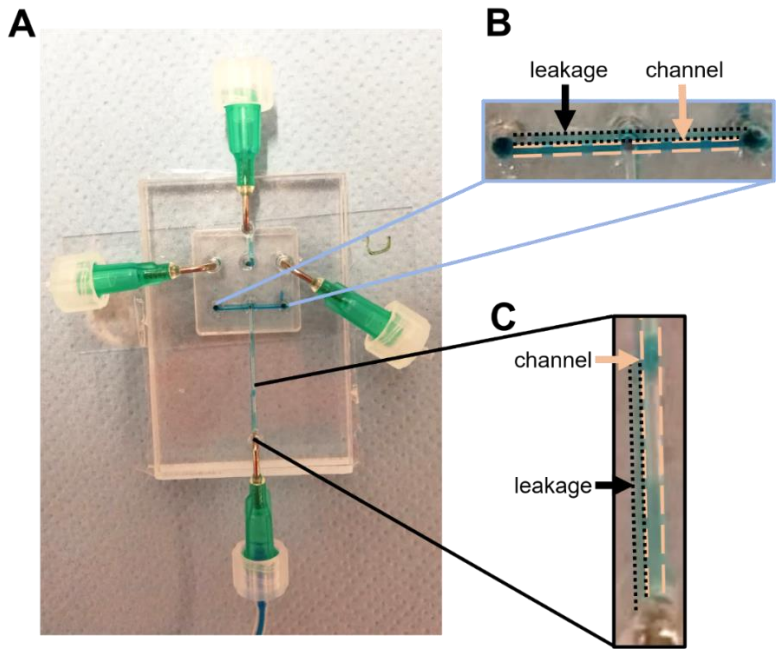

Figure 12: ***Food*** **color** ***pushed through mini-FCB and chip.*** *A) Leakage can be observed where the adhesive tape is cut for the channels and inlets. B), C) Zoom in on food* color *leakage.*

5.4 Comparing success rates of VFP

In the BvoCs used for the first fluid flow experiment, VFP was successful in 12 out of 18 channels. VFP was considered successful if the channel did not collapse (see Figure 13 B and C, intact vs. collapsed lumen, respectively). The second time, VFP was successful in 11 out of 18 channels. The third time performed, in 18 out of 18 channels, besides having air bubbles captured in the collagen, VFP was successful. The lumen did not collapse. Success rates of 66.66%, 61.11%, and 100% were observed for VFP, the first, second, and third time performed, respectively, indicating that more experienced handling increases the success rate.

5.5 Studying the effect of fluid flow

Testing the effect of fluid flow on VFP BvoCs with and without HUVECs was used as an interim experiment to test the interfacing method using blunt needles.

5.5.1 Fluid flow through VFP BvoCs

The influence of fluid flow on the VFP lumen was tested. The mini-FCB with the chip inserted was connected via tubing to a syringe pump. A flow rate of 400 µl/min was used, yielding a shear of 3.1 Pa. Figure 13 shows an example of what is defined as an intact and what as a collapsed lumen (B and C, respectively). Having an intact lumen, the channel is lined with collagen, and fluid flow is possible. In a channel with a collapsed lumen, collagen (partially) fills the channel, and fluid flow is (partially) blocked. Picture D and E in Figure 13 show that the fluid flow has no visual influence on the lumen structure.

In the first experiment, in 2 out of 4 channels, fluid flow was observed, i.e., in the 4 channels tested, on 2 channels, the fluid flow had no visible impact on the stability of the VFP lumen. The second time performed, in 9 out of 11 channels, the flow had no visible impact on the stability of the VFP lumen. Therefore, the success rate of fluid flow was 50% for the first fluid flow experiment and 81.82% for the second time performed, indicating that fluid flow had no visible effect on the integrity of the lumen and that more experienced handling increases the success rate.

5.5.2 Fluid flow through VFP BvoCs seeded with HUVECs

To examine whether the cells would stay attached to the collagen lumen, a first fluid flow experiment was performed on VFP chips seeded with HUVECs. The mini-FCB with the chip inserted was connected via tubing to a syringe pump, and a flow velocity of 400 µl/min was used (shear of 3.1 Pa). In 8 out of 9 channels, flow was observed, and the success rate for fluid flow through VFP channels seeded with HUVECs was 88.88%. As shown in Figure 13 and in Videos (see Appendix Figure 20 and Figure 21 for QR codes), most cells remained attached to the lumen after exposure to a shear of 3.1 Pa. However, the HUVECs seeded in the channels did not form a uniform monolayer. Comparing the images before and after fluid flow, it seems that fluid flow had an effect on the integrity of the cells to the lumen.

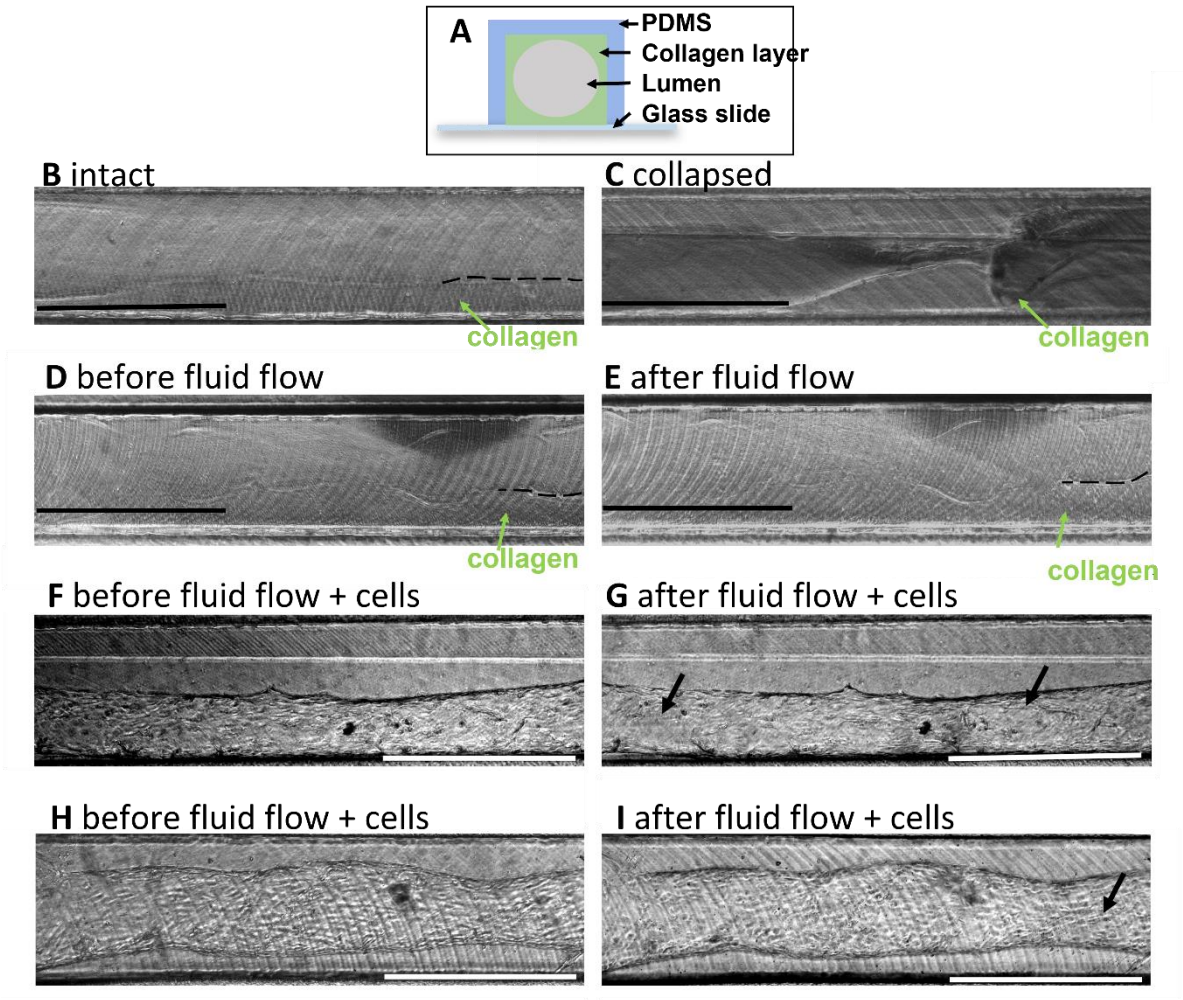

*Figure 13: **VFP lumen of the BvoCs.** A) Principle of VFP channel construction (not to scale). B) An intact lumen where collagen lines the channel in a finger-like shape. C) A collapsed lumen where collagen fills the channel. D) VFP channel before fluid flow. E) VFP channel after fluid flow. F), H) VFP channels seeded with HUVECs before fluid flow. G), I) VFP channels seeded with HUVECs after fluid flow was performed. A flow rate of 400 µl/min was used. Scale bar 700 µm.*

6. Discussion

In the following paragraphs, the design choices of the FCB and the results obtained are further analysed, discussed, and compared with literature.

6.1 Testing the interface between the BvoCs and the mini-FCB

The project´s challenge was to interface VFP BvoCs with FCBs. To test the interface, a mini-FCB was designed and developed, and blunt needles were used to attach the VFP BvoCs to the mini-FCB. De Graaf et al.[29], who connected VFP BvoCs to a FCB, used Luer locks, but they require a more complicated SolidWorks design for the inlets of the mini-FCB compared to the straight inlets required for blunt needles. Next, it has been hypothesized that the use of O-rings would increase the likelihood of damaging the VFP lumen due to a larger contact area with the PDMS. To maintain intact VFP lumen, the PDMS should be touched as little as possible. These considerations led to the choice of blunt needles, and the results show that using blunt needles to interface the BvoCs with the mini-FCB does not damage the VFP lumens. In addition, only minimal leakage was observed at the inlets, indicating that blunt needles allow a good connection between the BvoCs and the mini-FCB. However, when introducing flow, it was observed that in some channels where the fluid flow was blocked, the blunt needles and inlets did not align well. To improve the interfacing method, pillars could be added to the chip mould design. When pouring PDMS in the mould, the areas where the pillars are would stay PDMS-free and, after curing, would serve as inlets. Predefined inlets would result in a better fit of the chip in the chip pocket and increase the chance of successful fluid flow. Adjustments to the current SolidWorks design are easily made, and the fabrication steps will not change.

Gluing the blunt needles to the mini-FCB was successful when placing the PMMA plates on a flat surface while curing. To eliminate the adhesive's curing time and accelerate the fabrication, the needles could be pushed into the inlets instead of hammering or gluing. This method was successfully tested for a different microfluidic device by the research group AST. To use this method, a suitable diameter ratio between needles and inlets must be found that allows pushing needles into the inlets allowing for a tight fit and without causing cracks.

Needles with an OD of 0.81 mm got squeezed when separating the plastic hub from the steel needle. Another method to separate steel needle and plastic hub could be dissolving the glue with which the plastic hub is glued to the steel needle. This can be achieved by placing the blunt needle in ethanol. Steel needles could also be bought with the desired OD.[59]

6.2 Testing the bonding efficiency

To connect the top and bottom parts of the mini-FCB, adhesive bonding was performed. Previously designed FCBs, were connected by solvent bonding, but solvent bonding is, compared to adhesive bonding, time-consuming and requires the usage of chemicals.[27], [29] Using adhesive bonding resulted in a fast fabrication of the mini-FCB without the need for other equipment and specific knowledge. The number of air bubbles observed between the adhesive tape and the PMMA plates was reduced with practice. To further reduce bubbles, a manual scraper press, and hot press could be used.[60]

Minimal leakage was observed where the tape was cut for channels and inlets. Solvent bonding could be performed to eliminate the possibility of bubble formation in the tape and additionally reduce or even eliminate leakage at the channels. This bonding method is used for previously developed FCBs.[26], [27], [29] Using adhesive bonding, the adhesive tape has to be cut for channels and inlets, resulting in areas of uneven bonding which is not the case for solvent bonding. With solvent bonding, the plates are bonded together evenly. Therefore, it is hypothesized that solvent bonding could give

better results. However, testing this was too time-consuming for the extent of this study. Moreover, since chemicals are required, a company could perform this method in future studies.

6.3 Testing fluid flow through VFP BvoCs and VFP BvoCs seeded with HUVECs

During this project, VFP was performed to create collagen-based 3D lumen on microfluidic chips. On average, the success rate for VFP was 63.89% for the experiments without cells and 100% for the experiments with cells seeded in the channel. The success rate for VFP increased over time, mainly due to better knowledge of the collagen behaviour and more experienced handling, which led to a faster workflow. Reasons for channel failure were the usage of pipet tips that were no longer cold enough, the usage of an old collagen-1 batch, an incorrect ratio of the collagen master mix, and slow working speed. The results show that experienced handling increases the VFP success rates. Since the number of VFP experiments performed is low (n=3), it is believed that with further practice, the repeatability for VFP will be relatively high. However, the calculated success rates were only based on perfusable lumen, where the collagen did not collapse. The lumen diameter was not analysed during this project, but variations on this result in ECs experiencing different WSS.[29] For future experiments, the variation in lumen diameter should be reduced to keep the WSS more consistent. Lumen diameter can be controlled by the volume of the driving fluid, the collagen concentration, and the driving pressure.[15], [29] De Graaf et al.[29] recently published a method to reduce the influence that variations in lumen diameter have on the WSS. In this study, a FCB was designed for controlled perfusion of 3D BvoCs that accounts for diameter variability by adding an extra hydraulic resistance next to the hydraulic resistance of the BvoC channels. Using this approach in future research increases the throughput since the WSS variability resulting from different diameters is reduced.

Next, fluid flow experiments were performed to test whether VFP lumen would remain intact when introducing flow. This was an interim experiment to check whether it could be continued with the developed interfacing method. The results show that introducing flow on VFP BvoC did not seem to affect the lumen integrity (average success rate = 65.91%). In some channels, fluid could not flow due to collapsed collagen blocking the fluid flow (see Figure 13 C). Since the focus of this project was not on optimizing the VFP method and the amount of VFP performed is relatively low, it is difficult to analyse the reproducibility of this method. However, Graaf et al.[29] optimized VFP using a different hydrogel composition and a syringe to inject the hydrogel into the channel via pipet tips. Whether these adjustments increase the reproducibility of the VFP method should be tested in future studies.

Considering the experiments with cells, fluid flow success rates were higher for the chips with cells compared to those without cells (88.88% with cells vs. 50% and 81.82% without cells). This could be due to the cells giving better stability to the lumen since, in blood vessels, they form a barrier between blood and tissues.[55] Also, more experienced handling increases the success rate. However, more experiments must be performed to draw a statistically correct conclusion. In addition, it was observed that the HUVECs seeded on VFP BvoCs did not form a uniform monolayer after two days of culture (see Figure 13). Moreover, fluid flow did affect the monolayer, as shown in Figure 13, where fewer cells lined the channels after fluid flow was introduced. One reason for inconsistent monolayer and unstable cell-lumen integrity may be the high passage number of the cells used (passage 9). From passage 4 on, HUVECs have a higher doubling time and show decreased proliferation, and after passage 6 HUVECs lose their ability to adapt to stresses.[61], [62] Another reason may be the fact that cell seeding and culturing were performed under static conditions. For future experiments, it is suggested to place the chips on a slow rotator upon seeding to allow uniform cell attachment around the whole lumen, as tested by de Graaf et al.[15], [29]. As explained earlier, adding flow is an indispensable requirement for BvoCs to resemble human physiology more closely. However, since cells experience sudden stress when higher flow rates are introduced, the sudden introduction of high flow rates during this study

may have resulted in cell detachment. Therefore, it is recommended to start with lower flow rates and, after monolayer formation, gradually increase flow rates.[27] Next, in earlier experiments, it was observed that the cells showed a better morphology using different cell culture medium (EGM-2). However, since the fluid flow experiments were proof of principle experiments, EGM medium was used. In contrast to EGM, EGM-2 is supplemented with FBS and several growth factors promoting, among others, cell growth and proliferation, physical organization of ECs in tube-like structures, and angiogenesis, which could explain improved cell growth and morphology in experiments using EGM-2 medium. [63]–[65] For future experiments, it is advised to use EGM-2 medium.

During the experiments, a fluid flow of 400 µl/min was used, resulting in a shear stress of 3.1 Pa (eqn 2), which lies in the range found in human arteries (1-7 Pa)[31], [32]; thus, the cells experienced physiological shear. Therefore, the results of the fluid flow experiments give a first indication that the proposed interfacing would work to introduce flow on the BvoCs and that physiological shear does not destroy the lumen structure. Whether the lumen remains intact when using higher shear still needs to be determined. To ensure cell-lumen integrity when introducing flow, the above-mentioned recommendations should be tested in future research.

6.4 Trade-off between physiological shear and continuous flow on the VFP BvoCs

Since the Bossink pumps[40] require the same fabrication steps as pneumatic push-up valves, they were chosen for this FCB design for convenience. However, this pump design limits the flow rate to 48 µl/min (shear stress of 0.37 Pa, eqn 2). Shear stresses found in arteries range between 1 and 7 Pa.[31], [32] Therefore, the shear stress the Bossink pump can obtain is 2.7-19 times lower than the shear stress in arteries.[66] To achieve a WSS of 1 Pa using the Bossink pump, a flow rate of 128 µl/min is needed (eqn 3), which is 2.67 times higher than the flow rate achieved with the current valve design of the Bossink pump (48 µl/min). To achieve a flow rate that is 2.67 times higher, the valve dimensions have to be 2.67 times higher resulting in a required width-height ratio of $5.33*10^{-7}m^2$ (eqn 5). New valve dimensions could be, for example 410 µm x 1300 µm (height x width). In future experiments, it should be tested whether these valve dimensions could achieve a flow rate of 128 µl/min and whether the flow channel can be closed off properly. If the valve cannot achieve the desired flow rate with the new dimensions, a trade-off could be made not to achieve *in vivo* shear stress but to have continuous flow and allow for parallelization.

6.5 Throughput and widespread use

One of the aims of OoC research is high-throughput and widespread use. In general, the results suggest that using blunt needles for interfacing is suitable for widespread use as no specific knowledge is required to make and use the mini-FCB. To increase the throughput, it is recommended to test pushing blunt needles in the inlets as described above since this reduces fabrication time. Next, adding predefined inlets to the chip mould allows for a better connection between the chip inlets and the blunt needles in the chip pocket. However, before this method can be scaled up, leakage observed at channels needs to be eliminated and cell-lumen integrity has to be improved.

With the designed FCB, experiments on three BvoCs (9 channels) can be performed simultaneously. When micro-milling several FCBs, more experiments could be performed at the same time. The limiting factor is the need for a setup with external solenoid valves and incubators, as well as the need for LabVIEW to make automatic cell culture possible.

Applying the mentioned improvements and using micro-milling to enable fast fabrication of semi-circular flow channels makes the designed FCB and modular BBs more attractive for widespread use. However, to make widespread use of the designed FCB and the BBs possible, it must be tested whether

the FCB and the BBs work as proposed. If this succeeds, the standardization approach can enable cooperation between research groups and companies and thus facilitate widespread use. [25], [29]

6.6 Recommendations

6.6.1 Introducing continuous flow and reperfusion on BvoCs

To meet the requirements of introducing continuous flow and reperfusion on BvoCs, push-up valves, and Bossink pumps were integrated into BB1, 2, and 4 of the FCB design. The low bulkiness, low cost, and easy integration into soft-lithography designs make this type of valve and pump the preferred choice. However, push-up valves require semi-circular flow channels for the membrane to close the channel and stop fluid flow.[23] During this project, a technique from literature was tested to create semi-circular flow channels. This technique was based on the surface tension of liquid PDMS.[67] However, the results show low reproducibility of the technique, for which reason they are not further discussed (see Appendix Figure 22). The research groups AST and BIOS have discovered a faster way to create semi-circular channels directly into the PMMA mould by micro-milling. Before, using micro-milling was time-consuming.[21] The calculation of the milling path took up to 8h and sometimes caused computer crashes. A new method has been found to design semi-circular flow channels in SolidWorks, reducing the time needed to calculate the milling path. Since this method was found towards the end of the project, it could not be tested but the results found by the research groups look promising, and the use of micro-milling to create semi-circular flow channels is therefore recommended for future work.

6.6.2 Using ECs in combination with VSMCs to resemble the *in vivo* lumen structure more closely and improve lumen integrity

Cuenca et al.[17] discovered irregular monolayer formation when using only hiPSC-ECs. Including VSMCs in the BvoC model resembles the human vessel structure more closely and could result in better integrity of the ECs to the lumen since VSMCs support ECs mechanically. Because the communication between ECs and VSMCs is essential for proper blood vessel function and divergent communication can result in vascular diseases, including VSMCs would improve the BvoC model. [17], [29], [68]

6.6.3 Using stem cells to test patient's reactions to drugs

In future experiments, incorporating stem cells into BvoC models could be considered. HUVECs have the disadvantage of limited availability and donor-to-donor variability but induced pluripotent stem cells (iPSCs) can be differentiated into any cell type and have the capacity for unlimited self-renewal.[17], [69] As Cuenca et al.[17] state, iPSCs have the genetic background of the donor from which they originate, and genetic diseases can be modelled using cells derived from patients. Using iPSCs could further help understand how plaque development progresses. Also, patient-specific drug responses could be investigated. With this, research will get closer to personalized medicine, enabling medical professionals to provide patients a better fitting therapy and reducing the amount of treatment failure and side effects.

Table of requirements for a realistic BvoC model comparing the current model, the proposed FCB model and the new state-of-the-art

Table 2 shows the previous state-of-the-art of the BvoC model and the FCB, the proposed FCB design, and the state-of-the-art at the end of this project.

Table 2: Table of requirements that a realistic BvoC model has to meet comparing the state-of-the-art before and after this project.

Requirements	**Definition**	**Previous state-of-the-art**		**BvoCs on a FCB**	
		VFP BvoC model	**FCB**	**Proposed design**	**New state-of-the-art**
3D	Round, collagen lumen	VFP	VFP [29]	VFP	VFP
Continuous flow		Rocking Plate	Pressure pump [27]	Peristaltic PDMS pump [21]	Interfacing works
***In vivo* shear stress**	1-7 Pa [31]	Pipet	Pressure pump [27]	Peristaltic PDMS pump [21]	
Recirculation of fluid	Unidirectional	Static	Solenoid and push-up valves [27]	Push-up valves	Interfacing works
Parallelization	Integrating multiple chips on one platform [25]	1 chip with 3 channels	12 VFP channels on one FCB [29]	3 chips with each 3 channels	Interfacing works
Long-term cell culture	8 days [56]	5 days	5 days [27]	By integrating new features – getting closer to in vivo	2 days, static cell culture conditions
Multiple cell types	HUVECs and VSMCs [17]	1 cell type (HUVECs)	Not yet tested with FCB	Future experiments	1 cell type (HUVECs)

7. Conclusion

The goal of this research project was to design a FCB that combines continuous reperfusion on parallelized 3D VFP BvoCs with physiological shear to bring the BvoC model to a higher level.

The presented design of the FCB with modular BBs combines standardization and modularity with ideas to introduce continuous recirculating flow on 3D VFP BvoCs, partial medium refreshment, and parallelization of experiments of up to three chips. To meet the requirements of introducing continuous reperfusion on parallelized 3D VFP BvoCs to capture the complexity of *in vivo* physiology better, a method had to be found to interface the BvoCs with the FCB and introduce flow on the chips while keeping the VFP lumen intact. To test the interface, a mini-FCB was designed and fabricated. Interfacing BvoCs with the mini-FCB using blunt needles was successful. Moreover, fluid flow was introduced on the BvoCs. The results show that the applied shear stress of 3.1 Pa did not affect the lumen integrity but the cell alignment. Performing the experiments repeatedly resulted in an increased success rate of fluid flow onto chips without collapsing lumen. The number of fluid flow experiments executed is low. Therefore, the success rate should increase even further after multiple fabrications of the interfacing method. However, to draw a statistically correct conclusion, more experiments must be performed. In addition, further optimization of the BBs allows interchangeability with other BBs designed according to ISO standards. This enables collaboration between different research groups as well as with companies. The designed FCB and modular BBs would allow a more straightforward setup of fluidic experiments with OoCs owing to reduced external connections and bulkiness.

Altogether, it is concluded that the FCB design could increase the relevancy of OoC-based technology in experimental studies with VFP blood vessels. The results show that OoCs with VFP channels, such as models to study CVD-related disease mechanisms and blood-brain barrier models, can be integrated into FCBs using blunt needles. Using this approach, research can get closer to the aim of reducing animal testing and enabling personalized medicine.

8. Acknowledgement

I would like to express my sincere gratitude to my daily supervisors, Heleen Goosen-Middelkamp MSc and Dr. Anke Vollertsen, who supported and motivated me a lot during all kinds of struggles I faced. I got a lot of tips and feedback that will help me in my future career. I have known both of them already for a couple of years and am glad that they were my supervisors during my Master's thesis. In addition, I would like to thank Prof. Dr. Andries van der Meer for being the head of my committee. He gave me practical tips during meetings and helped me during my writing process. I would also like to extend my appreciation to Prof. Dr. Ir. Mathieu Odijk and Prof. Dr. Ir. Séverine Le Gac for being my (external) supervisors and giving me support and constructive feedback and their time in evaluating my thesis.

Moreover, I would like to thank ir. Paul ter Braak, ir. Johan Bomer and Lisette Knippenborg for the technical support. A big thanks to Laura de Heus, Huub Weener, Eric Safai, Aniruddha Paul, and Dr. Elsbeth Bossink, who were always ready to help. Also, a big thanks to all other members of BIOS and AST for the coffee breaks, cakes, and group activities. Lastly, I would also like to thank all students, especially Britt Wesselink and Sabine de Winter for being my project buddies, Rianne Dalhuisen and Joyce Rops for their feedback and long hours in the library, as well as my housemate Wietske Rem who supported me a lot.

9. References

[1] "Cardiovascular diseases (CVDs)." [Online]. Available: https://www.who.int/en/news-room/fact-sheets/detail/cardiovascular-diseases-(cvds). [Accessed: 30-Sep-2022].

[2] L. Badimon, T. Padró, and G. Vilahur, "Atherosclerosis, platelets and thrombosis in acute ischaemic heart disease," *Eur. Hear. Journal. Acute Cardiovasc. Care*, vol. 1, no. 1, p. 60, Apr. 2012.

[3] Y. T. Lee *et al.*, "Mouse models of atherosclerosis: a historical perspective and recent advances," *Lipids Health Dis.*, vol. 16, no. 1, Jan. 2017.

[4] S. Jebari-Benslaiman *et al.*, "Pathophysiology of Atherosclerosis," *Int. J. Mol. Sci. 2022, Vol. 23, Page 3346*, vol. 23, no. 6, p. 3346, Mar. 2022.

[5] "Coronary artery disease - Knowledge @ AMBOSS." [Online]. Available: https://www.amboss.com/us/knowledge/Coronary_artery_disease. [Accessed: 26-Oct-2022].

[6] P. Golforoush, D. M. Yellon, and S. M. Davidson, "Mouse models of atherosclerosis and their suitability for the study of myocardial infarction," *Basic Res. Cardiol.*, vol. 115, no. 6, p. 73, Dec. 2020.

[7] C. Ma, Y. Peng, H. Li, and W. Chen, "Organ-on-a-Chip: A new paradigm for drug development," *Trends Pharmacol. Sci.*, vol. 42, no. 2, p. 119, Feb. 2021.

[8] H. Savoji *et al.*, "Cardiovascular disease models: A game changing paradigm in drug discovery and screening," *Biomaterials*, vol. 198, pp. 3–26, Apr. 2019.

[9] J. van der Velden *et al.*, "Animal models and animal-free innovations for cardiovascular research: current status and routes to be explored. Consensus document of the ESC Working Group on Myocardial Function and the ESC Working Group on Cellular Biology of the Heart," *Cardiovasc. Res.*, vol. 17, Jan. 2022.

[10] C. M. Leung *et al.*, "A guide to the organ-on-a-chip," *Nat. Rev. Methods Prim. 2022 21*, vol. 2, no. 1, pp. 1–29, May 2022.

[11] D. E. Ingber, "Human organs-on-chips for disease modelling, drug development and personalized medicine," *Nat. Rev. Genet. 2022 238*, vol. 23, no. 8, pp. 467–491, Mar. 2022.

[12] Q. Wu *et al.*, "Organ-on-a-chip: recent breakthroughs and future prospects," *Biomed. Eng. OnLine 2020 191*, vol. 19, no. 1, pp. 1–19, Feb. 2020.

[13] E. Delannoy, G. Tellier, J. Cholet, A. M. Leroy, A. Treizebré, and F. Soncin, "Multi-Layered Human Blood Vessels-on-Chip Design Using Double Viscous Finger Patterning," *Biomed. 2022, Vol. 10, Page 797*, vol. 10, no. 4, p. 797, Mar. 2022.

[14] P. F. Costa *et al.*, "Mimicking arterial thrombosis in a 3D-printed microfluidic in vitro vascular model based on computed tomography angiography data," *Lab Chip*, vol. 17, no. 16, pp. 2785–2792, Aug. 2017.

[15] M. N. S. De Graaf *et al.*, "Scalable microphysiological system to model three-dimensional blood vessels," *APL Bioeng.*, vol. 3, no. 2, p. 026105, Jun. 2019.

[16] E. Westein, A. D. Van Der Meer, M. J. E. Kuijpers, J. P. Frimat, A. Van Den Berg, and J. W. M. Heemskerk, "Atherosclerotic geometries exacerbate pathological thrombus formation poststenosis in a von Willebrand factor-dependent manner," *Proc. Natl. Acad. Sci. U. S. A.*, vol. 110, no. 4, pp. 1357–1362, Jan. 2013.

[17] M. Vila Cuenca *et al.*, "Engineered 3D vessel-on-chip using hiPSC-derived endothelial- and

vascular smooth muscle cells," *Stem Cell Reports*, vol. 16, no. 9, pp. 2159–2168, Sep. 2021.

[18] A. Herland, A. D. Van Der Meer, E. A. FitzGerald, T. E. Park, J. J. F. Sleeboom, and D. E. Ingber, "Distinct Contributions of Astrocytes and Pericytes to Neuroinflammation Identified in a 3D Human Blood-Brain Barrier on a Chip," *PLoS One*, vol. 11, no. 3, Mar. 2016.

[19] L. L. Bischel, S. H. Lee, and D. J. Beebe, "A Practical method for patterning lumens through ECM hydrogels via viscous finger patterning," *J. Lab. Autom.*, vol. 17, no. 2, pp. 96–103, Apr. 2012.

[20] M. C. Tsai, S. Y. Wei, L. Fang, and Y. C. Chen, "Viscous Fingering as a Rapid 3D Pattering Technique for Engineering Cell-Laden Vascular-Like Constructs," *Adv. Healthc. Mater.*, vol. 11, no. 1, p. 2101392, Jan. 2022.

[21] E. G. B. M. Bossink, A. R. Vollertsen, J. T. Loessberg-Zahl, A. D. Van Der Meer, L. I. Segerink, and M. Odijk, "Systematic characterization of cleanroom-free fabricated macrovalves, demonstrating pumps and mixers for automated fluid handling tuned for organ-on-chip applications."

[22] A. Polini and L. Moroni, "The convergence of high-tech emerging technologies into the next stage of organ-on-a-chips," *Biomater. Biosyst.*, vol. 1, p. 100012, Mar. 2021.

[23] J. Melin and S. R. Quake, "Microfluidic Large-Scale Integration: The Evolution of Design Rules for Biological Automation," 2007.

[24] S. Dekker *et al.*, "Standardized and modular microfluidic platform for fast Lab on Chip system development," *Sensors Actuators B*, vol. 269, pp. 468–478, 2018.

[25] A. R. Vollertsen, A. Vivas, B. van Meer, A. van den Berg, M. Odijk, and A. D. van der Meer, "Facilitating implementation of organs-on-chips by open platform technology," *Biomicrofluidics*, vol. 15, no. 5, p. 051301, Oct. 2021.

[26] A. R. Vollertsen *et al.*, "Modular operation of microfluidic chips for highly parallelized cell culture and liquid dosing via a fluidic circuit board," *Microsystems Nanoeng. 2020 61*, vol. 6, no. 1, pp. 1–16, Nov. 2020.

[27] A. Vivas, A. van den Berg, R. Passier, M. Odijk, and A. D. van der Meer, "Fluidic Circuit Board with Modular Sensor and Valves Enables Stand-Alone, Tubeless Microfluidic Flow Control in Organs-on-Chips," *bioRxiv*, p. 2021.11.24.469685, Nov. 2021.

[28] S. Dekker, P. K. Isgor, T. Feijten, L. I. Segerink, and M. Odijk, "From chip-in-a-lab to lab-on-a-chip: a portable Coulter counter using a modular platform," *Microsystems Nanoeng.*, vol. 4, no. 1, Dec. 2018.

[29] M. N. S. de Graaf *et al.*, "Multiplexed fluidic circuit board for controlled perfusion of 3D blood vessels-on-a-chip," *Lab Chip*, vol. 23, no. 1, pp. 168–181, Dec. 2022.

[30] E. G. B. M. Bossink, "Recreating the gut on-chip: Sensors and fabrication technologies for aerobic intestinal host – anaerobic microbiota research," Jul. 2022.

[31] E. Roux, P. Bougaran, P. Dufourcq, and T. Couffinhal, "Fluid Shear Stress Sensing by the Endothelial Layer," *Front. Physiol.*, vol. 11, p. 861, Jul. 2020.

[32] J. M. Dolan, J. Kolega, and H. Meng, "High Wall Shear Stress and Spatial Gradients in Vascular Pathology: A Review," *Ann. Biomed. Eng.*, vol. 41, no. 7, p. 1411, Jul. 2013.

[33] W. H. Montes and M. Molla, "BLOOD FLOW IN ARTERIES Related papers EXPERIMENTAL AND COMPUTAT IONAL MET HODS IN CARDIOVASCULAR FLUID MECHANICS T houfeek Hussain

Pulsat ile Non-Newt onian Fluid Flows in a Model Aneurysm wit h Oscillat ing Wall."

[34] M. R. Islam and M. E. Hossain, "State-of-the-art of drilling," *Drill. Eng.*, pp. 17–178, Jan. 2021.

[35] H. D. Goodfellow and E. F. Curd, "Physical fundamentals," *Ind. Vent. Des. Guideb.*, pp. 39–109, 2020.

[36] K. N. Asha and N. Srivastava, "Geometry of stenosis and its effects on the blood flow through an artery-A theoretical study," *AIP Conf. Proc.*, vol. 2375, Oct. 2021.

[37] "CV Physiology | Laminar Flow." [Online]. Available: https://www.cvphysiology.com/Hemodynamics/H006. [Accessed: 26-Oct-2022].

[38] J. Park and J. K. Park, "Integrated microfluidic pumps and valves operated by finger actuation," *Lab Chip*, vol. 19, no. 18, pp. 2973–2977, Sep. 2019.

[39] M. N. S. de Graaf, A. Vivas, A. D. van der Meer, C. L. Mummery, and V. V. Orlova, "Pressure-Driven Perfusion System to Control, Multiplex and Recirculate Cell Culture Medium for Organs-on-Chips," *Micromachines 2022, Vol. 13, Page 1359*, vol. 13, no. 8, p. 1359, Aug. 2022.

[40] E. GBM Bossink, A. R. Vollertsen, L. I. Segerink, A. D. van der Meer, and M. Odijk, "AUTOMATED MEDIUM RECIRCULATION USING MACRO VALVES FOR HIGH FLOW RATES IN AN ENDOTHELIAL CELL CULTURE CHIP."

[41] M. Mohammed *et al.*, "Studying the Response of Aortic Endothelial Cells under Pulsatile Flow Using a Compact Microfluidic System," *Anal. Chem.*, vol. 91, no. 18, pp. 12077–12084, Sep. 2019.

[42] T. Qian *et al.*, "Adaptable pulsatile flow generated from stem cell-derived cardiomyocytes using quantitative imaging-based signal transduction," *Lab Chip*, vol. 20, no. 20, pp. 3744–3756, Oct. 2020.

[43] J. Abello, Y. Y. Yien, and A. N. Stratman, "Adaptation of peristaltic pumps for laminar flow experiments," *bioRxiv*, p. 2021.10.17.464751, Oct. 2021.

[44] M. H. Wu, S. Bin Huang, Z. Cui, Z. Cui, and G. Bin Lee, "Development of perfusion-based micro 3-D cell culture platform and its application for high throughput drug testing," *Sensors Actuators B Chem.*, vol. 129, no. 1, pp. 231–240, Jan. 2008.

[45] S. Kondapalli and B. J. Kirby, "Refolding of β-galactosidase: Microfluidic device for reagent metering and mixing and quantification of refolding yield," *Microfluid. Nanofluidics*, vol. 7, no. 2, pp. 275–281, Jan. 2009.

[46] M. C. Cole, A. V. Desai, and P. J. A. Kenis, "Two-layer multiplexed peristaltic pumps for high-density integrated microfluidics," *Sensors Actuators B Chem.*, vol. 151, no. 2, pp. 384–393, Jan. 2011.

[47] R. Gómez-Sjöberg, A. A. Leyrat, D. M. Pirone, C. S. Chen, and S. R. Quake, "Versatile, fully automated, microfluidic cell culture system," *Anal. Chem.*, vol. 79, no. 22, pp. 8557–8563, Nov. 2007.

[48] M. A. Unger, H. P. Chou, T. Thorsen, A. Scherer, and S. R. Quake, "Monolithic microfabricated valves and pumps by multilayer soft lithography," *Science (80-.).*, vol. 288, no. 5463, pp. 113–116, Apr. 2000.

[49] A. L. Bowen and R. S. Martin, "Integration of on-chip peristaltic pumps and injection valves with microchip electrophoresis and electrochemical detection," *Electrophoresis*, vol. 31, no. 15, pp. 2534–2540, Aug. 2010.

[50] C. Zheng, X. Zhang, C. Li, Y. Pang, and Y. Huang, “Microfluidic Device for Studying Controllable Hydrodynamic Flow Induced Cellular Responses,” *Anal. Chem.*, vol. 89, no. 6, pp. 3710–3715, Mar. 2017.

[51] “Physiology Tutorial - Blood Flow.” [Online]. Available: http://www.vhlab.umn.edu/atlas/physiology-tutorial/blood-flow.shtml. [Accessed: 28-Nov-2022].

[52] P. Loskill, S. G. Marcus, A. Mathur, W. M. Reese, and K. E. Healy, “µOrgano: A Lego®-Like Plug & Play System for Modular Multi-Organ-Chips,” *PLoS One*, vol. 10, no. 10, p. e0139587, Oct. 2015.

[53] J. Rodriguez-Duarte *et al.*, “A novel nitroalkene-α-tocopherol analogue inhibits inflammation and ameliorates atherosclerosis in Apo E knockout mice,” *Br. J. Pharmacol.*, vol. 176, no. 6, pp. 757–772, Mar. 2019.

[54] W. Lu, X. He, L. Su, and J. Miao, “Long Noncoding RNA-CERNA1 Stabilized Atherosclerotic Plaques in apolipoprotein E −/− Mice,” *J. Cardiovasc. Transl. Res.*, vol. 12, no. 5, pp. 425–434, Oct. 2019.

[55] M. Ouarné, A. Pena, and C. A. Franco, “From remodeling to quiescence: The transformation of the vascular network,” *Cells Dev.*, vol. 168, p. 203735, Dec. 2021.

[56] I. Pediaditakis *et al.*, “Modeling alpha-synuclein pathology in a human brain-chip to assess blood-brain barrier disruption,” *Nat. Commun. 2021 121*, vol. 12, no. 1, pp. 1–17, Oct. 2021.

[57] S. R. A. Kratz *et al.*, “Characterization of four functional biocompatible pressure-sensitive adhesives for rapid prototyping of cell-based lab-on-a-chip and organ-on-a-chip systems,” *Sci. Rep.*, vol. 9, no. 1, Dec. 2019.

[58] “Product Information Sheet ARcare® 90106NB.”

[59] “Stainless Steel Straight Connector.” [Online]. Available: https://www.harvardapparatus.com/stainless-steel-straight-connector.html. [Accessed: 21-Feb-2023].

[60] C. W. Tsao and W. C. Syu, “Bonding of thermoplastic microfluidics by using dry adhesive tape,” *RSC Adv.*, vol. 10, no. 51, p. 30289, Aug. 2020.

[61] T. Osaki *et al.*, “Flatbed epi relief-contrast cellular monitoring system for stable cell culture,” *Sci. Rep.*, vol. 7, no. 1, Dec. 2017.

[62] D. J. Medina-Leyte, M. Domínguez-Pérez, I. Mercado, M. T. Villarreal-Molina, and L. Jacobo-Albavera, “Use of Human Umbilical Vein Endothelial Cells (HUVEC) as a Model to Study Cardiovascular Disease: A Review,” *Appl. Sci. 2020, Vol. 10, Page 938*, vol. 10, no. 3, p. 938, Jan. 2020.

[63] “EGM-2 Endothelial Cell Growth Medium-2 BulletKit, CC-3162 | Lonza.” [Online]. Available: https://bioscience.lonza.com/lonza_bs/NL/en/Primary-and-Stem-Cells/p/000000000000185303/EGM™-2-Endothelial-Cell-Growth-Medium-2-BulletKit™. [Accessed: 24-Feb-2023].

[64] “Endothelial Cell Media | Sterile Culture Medium | High Quality | Cell Applications.” [Online]. Available: https://www.cellapplications.com/human-endothelial-cell-media. [Accessed: 24-Feb-2023].

[65] H. Lee and K. T. Kang, “Advanced tube formation assay using human endothelial colony forming cells for in vitro evaluation of angiogenesis,” *Korean J. Physiol. Pharmacol.*, vol. 22,

no. 6, p. 705, Nov. 2018.

[66] M. Klarhöfer, B. Csapo, C. Balassy, J. C. Szeles, and E. Moser, “High-resolution blood flow velocity measurements in the human finger,” *Magn. Reson. Med.*, vol. 45, no. 4, pp. 716–719, Apr. 2001.

[67] K. Lee *et al.*, “Fabrication of round channels using the surface tension of PDMS and its application to a 3D serpentine mixer,” *J. Micromechanics Microengineering*, vol. 17, no. 8, p. 1533, Jul. 2007.

[68] V. Sorokin *et al.*, “Role of Vascular Smooth Muscle Cell Plasticity and Interactions in Vessel Wall Inflammation,” *Front. Immunol.*, vol. 11, p. 3053, Nov. 2020.

[69] S. Moradi *et al.*, “Research and therapy with induced pluripotent stem cells (iPSCs): social, legal, and ethical considerations,” *Stem Cell Res. Ther. 2019 101*, vol. 10, no. 1, pp. 1–13, Nov. 2019.

[70] “Row of Four 4.5 ml Tanks with Luer Interface & Cap - Fluidic 233 - microfluidic ChipShop.” [Online]. Available: https://www.microfluidic-chipshop.com/catalogue/accessories/liquid-storage/liquid-storage-tanks/row-of-four-4-5-ml-tanks-with-luer-interface-cap-fluidic-233/. [Accessed: 22-Feb-2023].

10. Appendix

10.1 Calculations

Calculations shear stress

The wall shear stress in chips during flow experiments was calculated using the following equation.[15]

$$T = \eta * \frac{32*Q}{\pi*D^3} \quad (2)$$

Where

- T is the shear stress (Pa)
- Ƞ the dynamic viscosity of fluid ($0.72*10^{-3}$ Pa.s for cell culture medium, $0.79*10^{-3}$ Pa.s for cell culture medium with serum, $3*10^{-3}$ for blood)
- Q is the flow rate ($6.67*10^{-9}$ m^3/s used in flow experiments, $0.8*10^{-9}$ m^3/s Bossink pump)
- D the channel diameter ($250*10^{-6}$ m)

Shear stress used in flow experiments:	31 dyne / cm^2	=	3.1 Pa
Shear stress when using Bossink pump:	3.7 dyne / cm^2	=	0.37 Pa
Shear stress in arteries [31], [32]:	10-70 dyne / cm^2	=	1-7 Pa

Shear stress in flow experiments when using medium with serum:	34.3 dyne / cm^2 = 3.43 Pa
Shear stress in flow experiments using blood:	130 dyne / cm^2 = 13 Pa
Shear stress using Bossink pump and blood:	15.6 dyne / cm^2 = 1.56 Pa

Calculations flow rate

Calculating the flow rate the Bossink pump has to generate to achieve a WSS of 1 Pa by rewriting calculation (2).

$$Q = \frac{T*\pi*D^3}{32\eta} \quad (3)$$

Where

- Q is the flow rate (m^3/s)
- T is the shear stress (1 Pa)
- Ƞ the dynamic viscosity of fluid ($0.72*10^{-3}$ Pa.s for cell culture medium)
- D the channel diameter ($250*10^{-6}$ m)

The calculated flow rate (Q) to generate a WSS of 1 Pa is $2.13*10^{-9}$ m^3/s, which is 128 µl/min.

Calculations valve dimensions

Calculating the flow velocity with the current Bossink pump dimensions ($2*10^{-4}$ m * $1*10^{-3}$m (height * width)) and flow rate ($0.8*10^{-9}$ m^3/s):

$$Q = H * v * W \quad (4)$$

Where

- Q is the flow rate (m^3/s)
- H is the valve height (m)
- v is the flow velocity (m/s)
- W is the valve width (m)

The calculated flow velocity (v) is 0.004 m/sec.

Calculating the width-height ratio of the valve to achieve a flow rate of $2.13*10^{-9}$ m^3/s assuming that the flow velocity is 0.004 m/sec. Rewriting calculation (4) gives the following equation:

$$\frac{Q}{v} = H * W \quad (5)$$

The calculated width-height ratio of the valve is $5.33*10^{-7}$ m^2, which is 533000 μm^2.

The valve dimensions of the Bossink pump (200 µm * 1000 µm) have a width-height ratio of $2*10^{-7}$ m^2.

10.2 Possible reservoirs for the FCB

Figure 14: Row of four 4.5 ml tanks – fluidic 233, with Luer interface and Cap from microfluidic ChipShop.[70]

10.3 Tables comparing valves and pumps for the integration in FCBs

Table 3: Comparing solenoid valves with quake valves and push-up valves with push-down valves.

	Solenoid valve	**Quake valve**	
		Push-up valve	**Push-down valve**
Costs	Expensive	Low	
Bulkiness	High	Low	
Knowledge required	Programming skills	Soft-lithography	
Integration into microfluidic devices	More difficult due to the required programming skills	Easy	
		Lower actuation pressure required	Higher actuation pressure required

		Taller flow channel	Limited flow channel height
Used (/designed) by	Vivas et al.	Vollertsen et al.	de Winter et al.

Table 4: Comparing Peristaltic on-chip pumps with syringe and pressure pumps.

	Syringe pump	**Pressure pump**	**Peristaltic pump**
	Off-chip pump	Off-chip pump	Off-chip and on-chip pump
Flow	Constant volumetric flow	Pulseless, stable flow	Pulsative flow due to rotary motion
			Inexpensive
	Oscillations due to stepper motor		Positive displacement
Time needed for setup	Fast setup	Fast setup	Requires manufacturing time
Disadvantage	Do not adjust pressure when channels are clogged		
Parallelization possibility	Limited	Limited	High when integrated into a microfluidic device
Bulkiness	High	High	Low when integrated into a microfluidic device
	Large culture medium to cell ratio		
Flow rate			Up to 48 µl/min

10.4 Adjustments of the mini-FCB

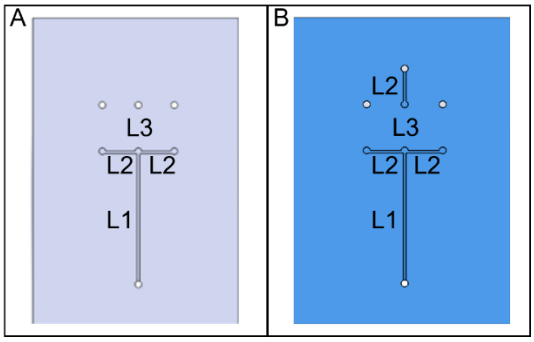

Figure 15: SolidWorks designs of the top part of the mini-FCB. A) First design of the top part. B) Second design of the top part with the middle outlet shifted upwards by L2.

10.5 Inlet diameters and blunt needle OD

Table 5: Inlet diameters of the top and bottom parts and the diameters of the blunt needles used.

Inlet diameter top part (mm)	**Blunt needle OD (mm)**	**Product number**
1.2 (glued) 1.3 (hammered)	1.27	918050-TE

Inlet diameter bottom part (mm)	Blunt needle OD (mm)	Product number
1.0 (glued)	0.81	921060-TE
1.0 (glued)	0.91	920050-TE
1.2 (hammered), 1.3 (glued)	1.27	918050-TE

10.7 Attaching blunt needles to the mini-FCB

Figure 16: Top part of mini-FCB where blunt needles went through the PMMA.

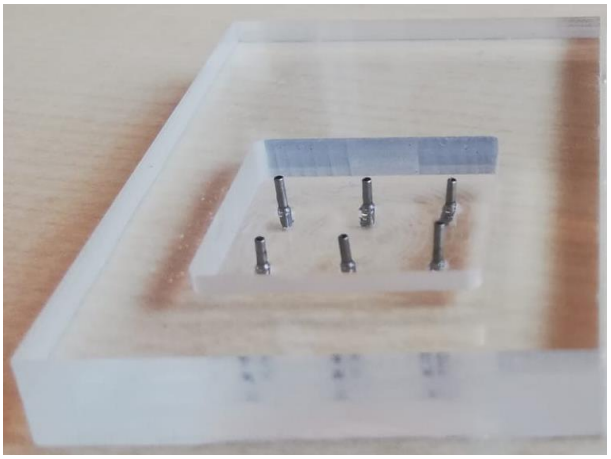

Figure 17: Small needles attached to the chip pocket became crooked when disconnecting the plastic hub from the steel needle

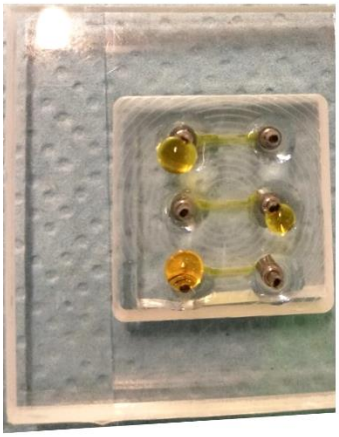

Figure 18: Showing fluid flow through the chip. The fluid enters the channels on one side and exits on the other. The chip was connected to the chip pocket via blunt needles (OD of 1.27 mm).

10.8 Fluid flow through BvoCs attached to the mini-FCB

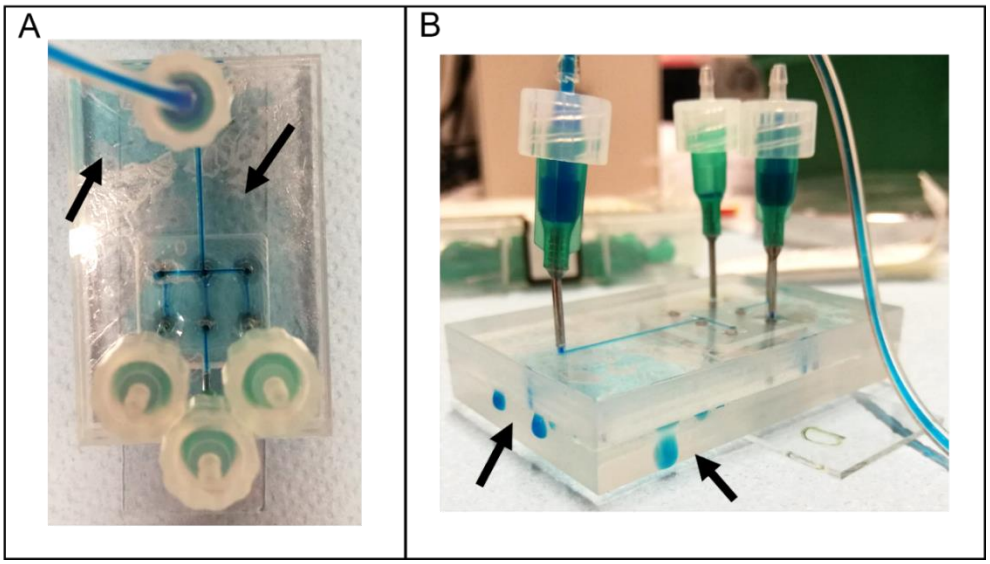

Figure 19: Food color *pushed through the chip via the mini-FCB. A) Bubbles in adhesive tape and food* color *leakage between the top and bottom plate. B) Food* color *leakage between the top and bottom parts.*

Videos of fluid flow experiments with cells

*Figure 20: QR code to a video showing fluid flow **in all three channels** of the VFP BvoC seeded with HUVECs.* As indicated in *Figure 13*, collagen lines the channel.

*Figure 21: QR code to a video showing fluid flow of **one channel** of a VFP BvoC seeded with HUVECs.* As indicated in *Figure 13*, collagen lines the channel.

10.9 Technique to create semi-circular flow channels using the surface tension of liquid PDMS

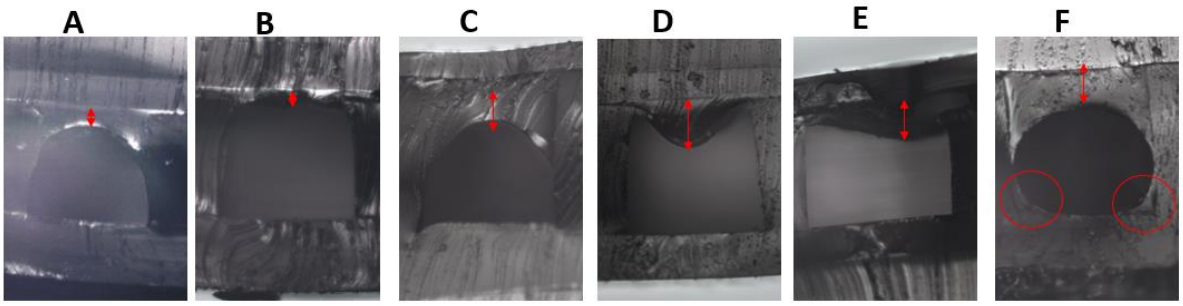

	A	B	C	D	E	F
Weight (g)	270	500	270	270	/	270
Degassing time (min)	/	/	40	30	20	40
Thickness (µm)	70	17	125	197	154	121

Figure 22: Cross-sections of BB1 and the settings used.